Journal of Computational Physics 461 (2022) 111199

Contents lists available at ScienceDirect

Journal of Computational Physics

www.elsevier.com/locate/jcp

Multi-symplectic discontinuous Galerkin methods for the stochastic Maxwell equations with additive noise

Jiawei Sun [a], Chi-Wang Shu [b,1], Yulong Xing [a,*,2]

[a] Department of Mathematics, The Ohio State University, Columbus, OH 43210, USA
[b] Division of Applied Mathematics, Brown University, Providence, RI 02912, USA

ARTICLE INFO

Article history:
Received 18 September 2021
Received in revised form 28 February 2022
Accepted 2 April 2022
Available online 22 April 2022

Keywords:
Discontinuous Galerkin methods
Stochastic Maxwell equations
Additive noise
Multi-symplectic method
Optimal error estimate

ABSTRACT

One- and multi-dimensional stochastic Maxwell equations with additive noise are considered in this paper. It is known that such system can be written in the multi-symplectic structure, and the stochastic energy increases linearly in time. High order discontinuous Galerkin methods are designed for the stochastic Maxwell equations with additive noise, and we show that the proposed methods satisfy the discrete form of the stochastic energy linear growth property and preserve the multi-symplectic structure on the discrete level. Optimal error estimate of the semi-discrete DG method is also analyzed. The fully discrete methods are obtained by coupling with symplectic temporal discretizations. One- and two-dimensional numerical results are provided to demonstrate the performance of the proposed methods, and optimal error estimates and linear growth of the discrete energy can be observed for all cases.

1. Introduction

In this paper we develop and analyze high order discontinuous Galerkin (DG) methods for one- and two-dimensional stochastic Maxwell equations with additive noise. Maxwell equations play an important role in many physical applications, and have been widely used in electromagnetism, electronic biology, optical imaging, etc. The general formulation of Maxwell equations is

$$\begin{cases} \partial_t \mathbf{D} = \nabla \times \mathbf{H} - \mathbf{J_e}, \quad \nabla \cdot \mathbf{D} = \rho, \\ \partial_t \mathbf{B} = -\nabla \times \mathbf{E}, \quad \nabla \cdot \mathbf{B} = \mathbf{0}, \end{cases} \tag{1.1}$$

where $\mathbf{H}$ represents the magnetic field, $\mathbf{E}$ stands for the electric field, $\mathbf{D}$ and $\mathbf{B}$ are the electric and magnetic flux density respectively. $\mathbf{J_e}$ is the electric current density, and ρ is the electric charge density.

Stochastic Maxwell equations are the generalized version of the deterministic Maxwell equations, which are often described as a random perturbation of the electric current density or the magnet current density by noise. The noises are commonly regarded as Brownian motion, Poisson process, etc. In [28], Rytov et al. introduced fluctuations of an electromagnetic field to obtain stochastic Maxwell equations. Ord showed in [26] that the random walk model due to Mark Kac can be

* Corresponding author.
E-mail addresses: sun.2261@buckeyemail.osu.edu (J. Sun), chi-wang_shu@brown.edu (C.-W. Shu), xing.205@osu.edu (Y. Xing).

[1] The work of this author is partially supported by NSF grant DMS-2010107 and AFOSR grant FA9550-20-1-0055.
[2] The work of this author is partially supported by the NSF grant DMS-1753581.

https://doi.org/10.1016/j.jcp.2022.111199
0021-9991/

modified to produce Maxwell's field equations in 1+1 dimensions. In [19], Liaskos et al. studied the stochastic integrodifferential equations in Hilbert spaces, and they examined the well posedness for the Cauchy problem of the integrodifferential equations describing Maxwell equations. The random electromagnetic fields using the spectral representation is explored in [18], and the electromagnetic fields were coupled by Maxwell equations with a random source term. Finite element approximations of a class of nonlinear stochastic wave equations with multiplicative noise were recently investigated in [17]. The semilinear stochastic Maxwell equations with additive noise in the following form:

$$\begin{cases} \epsilon d\mathbf{E} - \nabla \times \mathbf{H} dt = -\mathbf{J_e}(\mathbf{t}, \mathbf{x}, \mathbf{E}, \mathbf{H}) dt - \mathbf{J_e^r}(\mathbf{t}, \mathbf{x}) \circ dW, \\ \mu d\mathbf{H} + \nabla \times \mathbf{E} dt = -\mathbf{J_m}(\mathbf{t}, \mathbf{x}, \mathbf{E}, \mathbf{H}) dt - \mathbf{J_m^r}(\mathbf{t}, \mathbf{x}) \circ dW, \end{cases} \tag{1.2}$$

were studied by Chen et al. in [3], where dW is a space-time mixed color noise, more specifically, a Q-Wiener process which is often driven by Brownian motions, and $\mathbf{J_e}$ and $\mathbf{J_m}$ are described as electric current and magnetic current. Theoretical properties of the stochastic system (1.2) such as regularity, energy and divergence evolution law, and symplecticity have been presented in that paper. In addition, a stochastic Runge-Kutta semidiscretization scheme was proposed for (1.2) and proven to possess first order of mean accuracy. In [10], Cohen et al. developed an exponential integrator for a more generalized formulation of (1.2), when $\mathbf{J_e^r}$ and $\mathbf{J_m^r}$ depend on $\mathbf{E}$ and $\mathbf{H}$. In a recent review article, Zhang et al. [30] presented different types of stochastic Maxwell equations with additive or multiplicative noises.

Stochastic Maxwell equations can be viewed as a type of stochastic Hamiltonian PDEs. In [13], Jiang et al. considered stochastic Hamiltonian PDEs in the form

$$Mdz + Kz_x dt = \nabla_z S_1(z) dt + \nabla_z S_2(z) dW_t, \tag{1.3}$$

where M and K are anti-symmetric matrices, and S_1 and S_2 are smooth functions of z. It can be shown that the system (1.3) satisfies the following stochastic multi-symplectic conservation law:

$$d\omega + \partial_x \kappa dt = 0, \qquad \omega = MU \cdot V, \qquad \kappa = KU \cdot V,$$

which U and V are a pair of solutions to the variational equation

$$Md(\partial z) + K(\partial z)_x dt = \nabla_z^2 S_1(z) \partial z dt + \nabla_z^2 S_2(z) \partial z dW_t.$$

In [2,11], multi-symplectic finite difference methods have been studied for the stochastic Maxwell equations with additive noise of the form

$$\begin{cases} \epsilon d\mathbf{E} = \nabla \times \mathbf{H} dt - \lambda_1 \mathbf{1}^{\mathbf{T}} dW, \\ \mu d\mathbf{H} = -\nabla \times \mathbf{E} dt + \lambda_2 \mathbf{1}^{\mathbf{T}} dW, \end{cases} \tag{1.4}$$

with constant coefficient λ_1 and λ_2. This model can be reformulated in two slightly different formulations of (1.3) in [2,11] with different set of auxiliary variables introduced. Numerical methods based on these reformation have been presented and studied, and it was shown that these methods preserve stochastic multi-symplecticity on the discrete level. In addition, the linear growth property of stochastic energy was also preserved by the proposed methods. In [12], the extension to stochastic Maxwell equations with multiplicative noise was investigated. In a recent work [1], Chen developed a symplectic discontinuous Galerkin full discretization method for the system (1.4). The author presented H^k regularity ($k = 1, 2$) of the solutions to stochastic Maxwell equation, and showed the DG full discretization has the convergence order $k/2$ in time and $k - 1/2$ in space.

In this work, we investigate the high-order schemes for stochastic Maxwell equations, following the recent work in [15] on DG methods for stochastic conservation laws. The DG method is a class of finite element methods that uses discontinuous piecewise polynomials as the basis functions. This method has been shown to adopt many advantages from both finite element and finite volume methods, which includes hp-adaptivity flexibility, efficient parallel implementation, the ability of handling complicated boundary conditions, etc. The DG methods were first introduced in [27] by Reed and Hill to solve transport equations, and later they were extended to solve hyperbolic conservation laws by Cockburn et al. in [6–9]. There have been some recent studies in extending DG method for stochastic partial differential equations. In [15] Li et al. applied the DG method to the stochastic conservation laws with multiplicative noise

$$du + f(u)_x dt = g(x, t, u) dW_t.$$

In [16], they also proposed an ultra-weak DG method for the stochastic Korteweg-De Vries equations in the form

$$du = -(u_{xxx} + f(u)_x) dt + g(x, t, u) dW_t.$$

Optimal error estimate was proven for the semilinear equations, and numerically optimal convergence rate was also observed for many nonlinear cases.

In this paper we apply high order DG methods to stochastic Maxwell equations with additive noise (1.4) in one and two dimensions. The stochastic energy of the exact solutions are shown to satisfy the linear growth property, and we will demonstrate that the numerical solutions of the semi-discrete DG methods satisfy the similar energy law on the discrete level. When the standard Brownian motion W_t is considered, the exactly same semi-discrete energy law can be obtained. Following the error estimate for the deterministic Maxwell equations, we provide the optimal error estimate of the semi-discrete DG methods for the one- and two-dimensional stochastic Maxwell equations on cartesian meshes. Furthermore, multi-symplectic property of certain DG methods for the one-dimensional deterministic multi-symplectic Hamiltonian partial differential equations (HPDEs) of the form

$$Mz_t + Kz_x = \nabla_z S(z)$$

has been recently investigated in [24]. Following the idea, we will start by establishing the multi-symplectic structure of the stochastic Maxwell equations, and then prove that the DG methods with suitable numerical fluxes can preserve the multi-symplecticity. The resulting semi-discrete methods are combined with symplectic temporal discretization. Both first order symplectic Euler method and second order symplectic partitioned Runge-Kutta (PRK) method will be introduced and analyzed in this paper.

The structure of this paper is as follows. Section 2 provides theoretical results for one-dimensional stochastic Maxwell equations. We discuss the conservation of multi-symplecticity of our DG scheme, demonstrate the energy law of numerical solutions, and present the result on the optimal error estimate of the proposed semi-discrete methods. Section 3 provides the same theoretical results on DG methods for two-dimensional stochastic Maxwell equations. Temporal discretization is provided in section 4. We consider both symplectic Euler method and the second order symplectic PRK method. Numerical results in both one and two dimensions are provided in section 5 to validate the convergence rate and the linear energy growth property. Section 6 contains some conclusion remarks.

Throughout this paper, L^2 norm is denoted by $\|\cdot\|$, and C represents a generic positive constant independent of the spatial and temporal step size h and Δt, which can take different values in different cases. In general, W_t represents a Q-Wiener process defined on a given probability space $(\Omega, \mathcal{F}, \mathbb{P})$, which can be characterized as

$$W_t = W(t, \mathbf{x}, \omega) = \sum_{m=1}^{\infty} \sqrt{\gamma_m} e_m(\mathbf{x}) \mathcal{B}_m(t, \omega), \quad t \geq 0, \ \ \mathbf{x} \in \mathbb{R} \text{ or } \mathbb{R}^2, \tag{1.5}$$

where $\{e_m\}$ is an orthonormal basis of $L^2(\mathbb{D})$, with $\mathbb{D} \subset \mathbb{R}^d$, $d = 1, 2$. $\mathcal{Q} : L^2(\mathbb{D}) \to L^2(\mathbb{D})$ is a symmetric, non-negative, finite trace operator such that $Tr(\mathcal{Q}) < \infty$ and $\mathcal{Q} e_m = \gamma_m e_m$ with $\gamma_m > 0$. Furthermore, $\{\mathcal{B}_m\}$ is a sequence of independent standard Brownian motions.

2. One-dimensional Maxwell equation with additive noise

In this section, the one-dimensional computational domain is denoted by I, which is partitioned into subintervals $I_j = [x_{j-\frac{1}{2}}, x_{j+\frac{1}{2}}]$ where $j = 1, 2, \cdots, N$. We also denote $x_j = \frac{1}{2}(x_{j-\frac{1}{2}} + x_{j+\frac{1}{2}})$ to be the center of each cell, and $h_j = x_{j+\frac{1}{2}} - x_{j-\frac{1}{2}}$ to be the mesh size. Let $h = \max_j h_j$ be the maximum mesh size. We further assume that h/h_j is bounded over all j during mesh refinement. Assume $P^k(I_j)$ to be the space of polynomials of degree up to k on I_j, and the piecewise polynomial space V_h^k is defined as follows:

$$V_h^k = \{v : v|_{I_j} \in P^k(I_j), \ \ j = 1, 2, \cdots, N\}.$$

Note that functions in V_h^k can be discontinuous at cell interfaces. Let $v^+_{j+\frac{1}{2}}$ and $v^-_{j+\frac{1}{2}}$ be the right and left limit of v at the interface $x_{j+\frac{1}{2}}$, and we denote by $\{v\}_{j+\frac{1}{2}} = \frac{1}{2}(v^+_{j+\frac{1}{2}} + v^-_{j+\frac{1}{2}})$ and $[v]_{j+\frac{1}{2}} = v^+_{j+\frac{1}{2}} - v^-_{j+\frac{1}{2}}$ the average and jump of v at $x_{j+\frac{1}{2}}$.

We start by considering the one-dimensional (1D) stochastic Maxwell equation with additive noise with periodic boundary condition of the form

$$\begin{cases} d\eta = -u_x dt - \lambda_1 dW_t, \\ du = -\eta_x dt + \lambda_2 dW_t, \end{cases} \tag{2.1}$$

which can be viewed as a 1D version of the model (1.4). The DG method with generalized fluxes for the deterministic version of (2.1) has been considered in [5,25], where the stability, error estimate and superconvergence properties have been studied. In this paper, the DG scheme for (2.1) is formulated as: for $x \in I$, $(\omega, t) \in \Omega \times [0, T]$, find $\eta_h(\omega, x, t), u_h(\omega, x, t) \in V_h^k$, such that for any test functions $\varphi, \widetilde{\varphi} \in V_h^k$, it holds that

$$\int_{I_j} d\eta_h \varphi(x) dx = \Big(\int_{I_j} u_h \varphi_x dx - (\breve{u}_h \varphi^-)_{j+\frac{1}{2}} + (\breve{u}_h \varphi^+)_{j-\frac{1}{2}} \Big) dt - \int_{I_j} \lambda_1 \varphi dW_t dx, \tag{2.2}$$

$$\int_{I_j} du_h\widetilde{\varphi}(x)dx = \Big(\int_{I_j} \eta_h\widetilde{\varphi}_x dx - (\breve{\eta}_h\widetilde{\varphi}^-)_{j+\frac{1}{2}} + (\breve{\eta}_h\widetilde{\varphi}^+)_{j-\frac{1}{2}}\Big)dt + \int_{I_j} \lambda_2\widetilde{\varphi}dW_t dx, \tag{2.3}$$

where the generalized alternating numerical fluxes are chosen to be

$$\breve{u}_h = \{u_h\} + \alpha[u_h], \qquad \breve{\eta}_h = \{\eta_h\} - \alpha[\eta_h],$$

for some non-zero constant $\alpha \in [-1, 1]$. Below, we will explore some theoretical properties of this DG method, including the semi-discrete energy law, optimal error estimate and the multi-symplectic structure.

2.1. Semi-discrete energy law

The exact solutions of the three dimensional stochastic Maxwell equation (1.4) satisfy the linear energy growth property, as studied in [11]. Below, we start by presenting similar result for the one-dimensional model (2.1).

Theorem 2.1 (***Continuous energy law***). *Let u and η be the solutions to the model (2.1) under periodic boundary condition. Denote the energy by $\mathcal{E}(t) = \int_I u^2(x,t) + \eta^2(x,t)dx$, then for any t, the global stochastic energy satisfies the following energy law*

$$\mathcal{E}(t) = \mathcal{E}(0) + 2\int_0^t \int_I (\lambda_2\eta - \lambda_1 u)dW_t dx + (\lambda_1^2 + \lambda_2^2)Tr(\mathcal{Q})t, \tag{2.4}$$

and, after taking the expectation,

$$\mathbb{E}\big(\mathcal{E}(t)\big) = \mathcal{E}(0) + (\lambda_1^2 + \lambda_2^2)Tr(\mathcal{Q})t. \tag{2.5}$$

Proof. By utilizing the Itô's lemma and the equations (2.1), we have

$$\begin{aligned} d\mathcal{E}(t) &= \int_I \big(2udu + 2\eta d\eta + d\langle u,u\rangle_t + d\langle \eta,\eta\rangle_t\big)dx \\ &= -\int_I (2u\eta_x + 2\eta u_x)dtdx + 2\int_I (\lambda_2 u - \lambda_1\eta)dW_t dx + (\lambda_1^2+\lambda_2^2)\int_I d\langle W_t, W_t\rangle_t dx. \end{aligned} \tag{2.6}$$

It follows from the periodic boundary condition and the definition of W_t that

$$\int_I (2u\eta_x + 2\eta u_x)dtdx = 0, \qquad \int_I d\langle W_t, W_t\rangle_t dx = Tr(\mathcal{Q})dt.$$

Therefore, (2.6) reduces to

$$d\mathcal{E}(t) = 2\int_I (\lambda_2 u - \lambda_1\eta)dW_t dx + (\lambda_1^2+\lambda_2^2)Tr(\mathcal{Q})dt. \tag{2.7}$$

Integrating (2.7) over t yields (2.4), and taking an expectation leads to (2.5). □

Next, we show that the following semi-discrete energy law is satisfied by the numerical solutions of the DG methods.

Theorem 2.2 (***Semi-discrete energy law***). *Let $u_h(\omega,x,t)$ and $\eta_h(\omega,x,t)$ be the numerical solutions to the DG methods (2.2) and (2.3).*
(a): For any $t \in [0,T]$, the numerical solutions satisfy the semi-discrete energy law

$$\begin{aligned} &\|u_h(\omega,x,t)\|^2 + \|\eta_h(\omega,x,t)\|^2 \\ &\quad = 2\int_0^t \int_I (\lambda_2 u_h - \lambda_1\eta_h)dW_s dx + \|u_h(x,0)\|^2 + \|\eta_h(x,0)\|^2 + (\lambda_1^2+\lambda_2^2)Kt, \end{aligned} \tag{2.8}$$

and

$$\mathbb{E}\Big(\|u_h(\omega,x,t)\|^2 + \|\eta_h(\omega,x,t)\|^2\Big) = \|u_h(x,0)\|^2 + \|\eta_h(x,0)\|^2 + (\lambda_1^2+\lambda_2^2)Kt, \tag{2.9}$$

with

$$K=\sum_{j=1}^{N}\sum_{l=0}^{k}\mu_j^l\sum_{m=1}^{\infty}\Big(\int_{I_j}\phi_j^l\sqrt{\gamma_m}e_m dx\Big)^2, \tag{2.10}$$

where $\{\phi_j^l,\ j=0,\cdots,k\}$ *represents the set of orthogonal Legendre basis over cell* I_j, *and* $\mu_j^l=(\int_{I_j}(\phi_j^l)^2dx)^{-1}$.
(b) The constant K *is bounded by* $(k+1)Tr(\mathcal{Q})$ *with* k *being the polynomial degree of the DG methods. Moreover, if there exists some constant* $\nu\in(0,2)$ *such that the series* $\sum_{m=1}^{\infty}\gamma_m(K_m)^{\nu}<\infty$ *with* $K_m=\|(e_m)_x\|_{\infty}$, *we can show that* $K=Tr(\mathcal{Q})+O(h^{\nu})$, *i.e., K is an approximation of* $Tr(\mathcal{Q})$ *appearing in the continuous energy law (2.4)-(2.5).*

Proof. (a): From Itô's formula, we have

$$d(u_h)^2=2u_h du_h+d\langle u_h,u_h\rangle_t,\qquad d(\eta_h)^2=2\eta_h d\eta_h+d\langle\eta_h,\eta_h\rangle_t. \tag{2.11}$$

By taking the test functions $\varphi=\eta_h$ and $\widetilde{\varphi}=u_h$ in the DG methods (2.2)-(2.3), and summing the resulting equations up, we have

$$\begin{aligned}\int_{I_j}((du_h)u_h+(d\eta_h)\eta_h)dx&=\int_{I_j}(\lambda_2u_h-\lambda_1\eta_h)dW_t dx+\Big(\int_{I_j}u_h(\eta_h)_x dx+\eta_h(u_h)_x dx\Big)dt\\&\quad+\Big(-\big((\{u_h\}+\alpha[u_h])\eta_h^-\big)_{j+\frac12}+\big((\{u_h\}+\alpha[u_h])\eta_h^+\big)_{j-\frac12}\Big)dt\\&\quad+\Big(-\big((\{\eta_h\}-\alpha[\eta_h])u_h^-\big)_{j+\frac12}+\big((\{\eta_h\}-\alpha[\eta_h])u_h^+\big)_{j-\frac12}\Big)dt\\&=-\Theta_{j+\frac12}+\Theta_{j-\frac12}+\int_{I_j}(\lambda_2u_h-\lambda_1\eta_h)dW_t dx,\end{aligned} \tag{2.12}$$

where

$$\Theta=\left(\frac12+\alpha\right)\eta_h^-u_h^+-\left(\frac12-\alpha\right)u_h^-\eta_h^+.$$

Let us represent the numerical solutions u_h in the cell I_j as

$$u_h(\omega,x,t)=\sum_{l=0}^{k}u_j^l(\omega,t)\phi_j^l(x),$$

which leads to

$$du_h=\sum_{l=0}^{k}du_j^l\phi_j^l.$$

Taking the test function $\widetilde{\varphi}=\phi_j^m$, $m=0,\cdots,k$, in (2.3), we obtain

$$\sum_{l=0}^{k}\Big(\int_{I_j}\phi_j^m\phi_j^l dx\Big)du_j^l=\mathcal{A}_j(\eta_h;\phi_j^m)dt+\int_{I_j}\lambda_2\phi_j^m dW_t dx \tag{2.13}$$

where the operator

$$\mathcal{A}_j(f;g)=\int_{I_j}fg_x dx-\big(\breve{f}g^-\big)_{j+\frac12}+\big(\breve{f}g^+\big)_{j-\frac12},$$

is introduced for ease of presentation. Denote the mass matrix by L_j with the (m,l) entry being $\int_{I_j}\phi_j^l\phi_j^m dx$. Note that the orthogonal Legendre basis are chosen, therefore L_j is a diagonal matrix, so is the inverse matrix L_j^{-1}. Let us denote $L_j^{-1}=\mathrm{diag}(\mu_j^0,\mu_j^1,\cdots,\mu_j^k)$ with $\mu_j^l=(\int_{I_j}(\phi_j^l)^2dx)^{-1}$. In addition, introduce the vectors

$$\mathbf{u}_j=\left(u_j^0,u_j^1\cdots,u_j^k\right)^T,\mathbf{A}_j=\left(\mathcal{A}_j(\eta_h;\phi_j^0),\mathcal{A}_j(\eta_h;\phi_j^1),\cdots,\mathcal{A}_j(\eta_h;\phi_j^k)\right)^T,\ \Phi_j=\left(\phi_j^0,\phi_j^1,\cdots,\phi_j^k\right)^T,$$

and the equation (2.13) can be rewritten as a linear system

$$L_j d\mathbf{u}_j = \mathbf{A}_j dt + \int_{I_j} \lambda_2 \Phi_j dW_t dx, \tag{2.14}$$

which leads to

$$d\mathbf{u}_j = L_j^{-1}\mathbf{A}_j dt + L_j^{-1}\int_{I_j} \lambda_2 \Phi_j dW_t dx. \tag{2.15}$$

It yields

$$du_j^l = \mu_j^l \mathcal{A}_j(\eta_h;\phi_j^l)dt + \mu_j^l\lambda_2 \int_{I_j} \phi_j^l \sum_m \sqrt{\gamma_m} e_m(x) dx d\mathcal{B}_m(t),$$

and furthermore we can obtain

$$d\langle u_j^l, u_j^l\rangle_t = \lambda_2^2 (\mu_j^l)^2 \sum_m \left(\int_{I_j} \phi_j^l \sqrt{\gamma_m} e_m(x) dx\right)^2 dt.$$

Therefore, we have

$$\begin{aligned}\int_{I_j} d\langle u_h, u_h\rangle_t dx &= \int_{I_j} d\Big\langle \sum_{l=0}^k u_j^l \phi_j^l, \sum_{l=0}^k u_j^l \phi_j^l \Big\rangle_t dx = \sum_{l=0}^k \left(\int_{I_j} \phi_j^l \phi_j^l dx\right) d\langle u_j^l, u_j^l\rangle_t \\ &= \lambda_2^2 \sum_{l=0}^k \mu_j^l \sum_m \left(\int_{I_j} \phi_j^l \sqrt{\gamma_m} e_m(x) dx\right)^2 dt. \end{aligned} \tag{2.16}$$

Similarly, we have

$$\int_{I_j} d\langle \eta_h, \eta_h\rangle_t dx = \lambda_1^2 \sum_{l=0}^k \mu_j^l \sum_m \left(\int_{I_j} \phi_j^l \sqrt{\gamma_m} e_m(x) dx\right)^2 dt. \tag{2.17}$$

The combination of (2.11), (2.12), (2.16) and (2.17) leads to

$$\begin{aligned}\int_{I_j} (d\langle u_h, u_h\rangle_t + d\langle \eta_h, \eta_h\rangle_t) dx =& -2\Theta_{j+\frac{1}{2}} + 2\Theta_{j-\frac{1}{2}} \\ &+ 2\int_{I_j} (\lambda_2 u_h - \lambda_1 \eta_h) dW_t dx + (\lambda_1^2 + \lambda_2^2) \sum_{l=0}^k \mu_j^l \sum_{m=1}^\infty \left(\int_{I_j} \phi_j^l \sqrt{\gamma_m} e_m dx\right)^2 dt. \end{aligned} \tag{2.18}$$

Summing over all the cells and integrating in time from 0 to t, we can obtain (2.8). Note that $\int_I (\lambda_2 u_h - \lambda_1 \eta_h) dW_s dx$ is an Itô integral, thus $\mathbb{E}\Big(\int_0^t \int_I (\lambda_2 u_h - \lambda_1 \eta_h) dW_s dx\Big) = 0$, and taking the expectation (2.8) leads to (2.9).

(b): For the constant K defined in (2.10), we can bound it by

$$\begin{aligned} K &\le \sum_{j=1}^N \sum_{l=0}^k \mu_j^l \sum_{m=1}^\infty \int_{I_j} (\phi_j^l)^2 dx \int_{I_j} \gamma_m e_m^2 dx = (k+1) \sum_{j=1}^N \sum_{m=1}^\infty \int_{I_j} \gamma_m e_m^2 dx \\ &= (k+1) \sum_{m=1}^\infty \int_I \gamma_m e_m^2 dx = (k+1) Tr(\mathcal{Q}), \end{aligned}$$

where $\mu_j^l = (\int_{I_j} (\phi_j^l)^2 dx)^{-1}$ is used.

Next, we show that K is an approximation of $Tr(\mathcal{Q})$. Note that $\phi_j^0 = 1$, $\mu_j^0 = 1/h_j$, and $\int_{I_j} \phi_j^l dx = 0$ for $l \ge 1$. Let us define $\overline{e}_m = \frac{1}{h_j}\int_{I_j} e_m dx$, and rewrite K as

$$K=\sum_{j=1}^{N}\sum_{m=1}^{\infty}\frac{\gamma_m}{h_j}\Big(\int_{I_j}e_m dx\Big)^2+\sum_{j=1}^{N}\sum_{m=1}^{\infty}\sum_{l=1}^{k}\mu_j^l\gamma_m\Big(\int_{I_j}\phi_j^l(e_m-\overline{e}_m)dx\Big)^2. \tag{2.19}$$

Using the fact that $Tr(\mathcal{Q})=\sum_{m=1}^{\infty}\gamma_m$ and $\sum_{j=1}^{N}\int_{I_j}e_m^2dx=1$, we have

$$\begin{aligned}K-Tr(\mathcal{Q})&=\sum_{j=1}^{N}\sum_{m=1}^{\infty}\gamma_m\left(\frac{1}{h_j}\Big(\int_{I_j}e_m dx\Big)^2-\int_{I_j}e_m^2dx\right)+\sum_{j=1}^{N}\sum_{m=1}^{\infty}\sum_{l=1}^{k}\mu_j^l\gamma_m\Big(\int_{I_j}\phi_j^l(e_m-\overline{e}_m)dx\Big)^2\\&=:I+II.\end{aligned} \tag{2.20}$$

Notice that

$$\int_{I_j}e_m^2dx=\int_{I_j}(e_m-\overline{e}_m+\overline{e}_m)^2dx=\int_{I_j}(e_m-\overline{e}_m)^2dx+\int_{I_j}\overline{e}_m^2dx=\int_{I_j}(e_m-\overline{e}_m)^2dx+\frac{1}{h_j}\Big(\int_{I_j}e_m dx\Big)^2,$$

which leads to

$$I=-\sum_{j=1}^{N}\sum_{m=1}^{\infty}\gamma_m\int_{I_j}(e_m-\overline{e}_m)^2dx.$$

Since e_m is uniformly bounded, there exists some constant M such that $|e_m-\overline{e}_m|^{2-\nu}\le M$, and we have the following estimate

$$\begin{aligned}|I|&=\sum_{j=1}^{N}\sum_{m=1}^{\infty}\gamma_m\int_{I_j}(e_m-\overline{e}_m)^2dx=\sum_{j=1}^{N}\sum_{m=1}^{\infty}\gamma_m\int_{I_j}|e_m-\overline{e}_m|^{\nu}|e_m-\overline{e}_m|^{2-\nu}dx\\&\le M\sum_{j=1}^{N}\sum_{m=1}^{\infty}\gamma_m\int_{I_j}|e_m-\overline{e}_m|^{\nu}dx\le M\sum_{j=1}^{N}\sum_{m=1}^{\infty}\gamma_m(K_m)^{\nu}h_j^{1+\nu}\\&=M\Big(\sum_{j=1}^{N}h_j^{1+\nu}\Big)\Big(\sum_{m=1}^{\infty}\gamma_m(K_m)^{\nu}\Big)=O(h^{\nu}),\end{aligned}$$

where $K_m=\|(e_m)_x\|_{\infty}$ and the assumption $\sum_{m=1}^{\infty}\gamma_m(K_m)^{\nu}<\infty$ is used. For the other term II, we can apply Young's inequality and follow the similar analysis as above to obtain

$$\begin{aligned}II&=\sum_{j=1}^{N}\sum_{m=1}^{\infty}\sum_{l=1}^{k}\mu_j^l\gamma_m\Big(\int_{I_j}\phi_j^l(e_m-\overline{e}_m)dx\Big)^2\le\sum_{j=1}^{N}\sum_{m=1}^{\infty}\sum_{l=1}^{k}\mu_j^l\gamma_m\int_{I_j}(\phi_j^l)^2dx\int_{I_j}(e_m-\overline{e}_m)^2dx\\&=\sum_{j=1}^{N}\sum_{m=1}^{\infty}\sum_{l=1}^{k}\gamma_m\int_{I_j}(e_m-\overline{e}_m)^2dx=k\sum_{j=1}^{N}\sum_{m=1}^{\infty}\gamma_m\int_{I_j}(e_m-\overline{e}_m)^2dx=O(h^{\nu}).\end{aligned}$$

The combination of these results lead to the conclusion that $K-Tr(\mathcal{Q})=O(h^{\nu})$, which finishes the proof. □

Remark 2.1. If W_t is the standard Brownian motion, we have $e_1=1$ and $e_m=0$ for $m>1$, therefore it can be easily shown that $I=II=0$ which leads to $K=Tr(\mathcal{Q})$. This means that the continuous energy law (2.4) is exactly preserved by the proposed method.

2.2. Optimal error estimates

The optimal error estimate analysis of the proposed semi-discrete DG method will be provided in this subsection.

We firstly define the generalized Radau $\mathcal{P}^{\alpha}$ projection operators which will be used in the analysis. On any cell I_j and for any function $g(x)$, its projection $\mathcal{P}^{\alpha}g$ into the space V_h^k is given by

$$\int_{I_j}(\mathcal{P}^{\alpha}g-g(x))v(x)dx=0,\ \forall v(x)\in P^{k-1}(I_j),\ \text{ and }(\{\mathcal{P}^{\alpha}g\}+\alpha[\mathcal{P}^{\alpha}g])_{j+\frac{1}{2}}=g(x_{j+\frac{1}{2}}). \tag{2.21}$$

The following property on the projection error is studied in [23,25] and will be used throughout this section.

Lemma 2.1 (***Projection error***). *Let $\mathcal{P}^\alpha$ (with $\alpha \neq 0$) be the generalized Radau projection defined above. For any smooth function $g(x) \in H^{k+1}$, there exists some constant C which is independent of h, such that*

$$\|\mathcal{P}^\alpha g - g\| \leq Ch^{k+1}\|g\|_{H^{k+1}}.$$

Theorem 2.3 (***Optimal error estimate***). *Let $u, \eta \in L^2(\Omega \times [0,T]; H^{k+2})$ be the strong solutions to the one-dimensional stochastic Maxwell equations with additive noise (2.1), and $u_h,\ \eta_h \in V_h^k$ be the numerical solutions given by the DG scheme (2.2) and (2.3). With the initial conditions chosen as*

$$\eta_h(x,0) = \mathcal{P}^{-\alpha}\eta(x,0),\ u_h(x,0) = \mathcal{P}^\alpha u(x,0),$$

and the assumption $\sum_m \gamma_m \|e_m\|^2_{H^{k+1}} < \infty$, there holds the following error estimate

$$\|u - u_h\|^2 + \|\eta - \eta_h\|^2 \leq Ch^{2k+2}. \tag{2.22}$$

Proof. Note that both the exact solution η and the numerical solution η_h satisfy the equation (2.2), and both u and u_h satisfy (2.3), therefore we have the following error equations

$$\int_{I_j} d(\eta - \eta_h)\varphi(x)dx = \Big(\int_{I_j}(u-u_h)\varphi_x dx - ((u-\breve{u}_h)\varphi^-)_{j+\frac{1}{2}} + ((u-\breve{u}_h)\varphi^+)_{j-\frac{1}{2}}\Big)dt, \tag{2.23}$$

$$\int_{I_j} d(u - u_h)\widetilde{\varphi}(x)dx = \Big(\int_{I_j}(\eta-\eta_h)\widetilde{\varphi}_x dx - ((\eta-\breve{\eta}_h)\widetilde{\varphi}^-)_{j+\frac{1}{2}} + ((\eta-\breve{\eta}_h)\widetilde{\varphi}^+)_{j-\frac{1}{2}}\Big)dt. \tag{2.24}$$

Let

$$\xi^\eta = \mathcal{P}^{-\alpha}\eta - \eta_h,\ \ \epsilon^\eta = \mathcal{P}^{-\alpha}\eta - \eta,\ \ \xi^u = \mathcal{P}^\alpha u - u_h,\ \ \epsilon^u = \mathcal{P}^\alpha u - u,$$

so that we can decompose the numerical error into two terms

$$\eta - \eta_h = \xi^\eta - \epsilon^\eta, \qquad u - u_h = \xi^u - \epsilon^u. \tag{2.25}$$

By choosing the test functions $\varphi = \xi^\eta$, $\widetilde{\varphi} = \xi^u$ in (2.23) and (2.24), and summing up the resulting equations, we obtain

$$\begin{aligned}
\int_{I_j}(d\xi^\eta\xi^\eta + d\xi^u\xi^u)dx = &\int_{I_j}(d\epsilon^\eta\xi^\eta + d\epsilon^u\xi^u)dx \\
&+ \Big(\int_{I_j}\xi^u\xi^\eta_x dx - \big((\{\xi^u\}+\alpha[\xi^u])(\xi^\eta)^-\big)_{j+\frac{1}{2}} + \big((\{\xi^u\}+\alpha[\xi^u])(\xi^\eta)^+\big)_{j-\frac{1}{2}}\Big)dt \\
&- \Big(\int_{I_j}\epsilon^u\xi^\eta_x dx - \big((\{\epsilon^u\}+\alpha[\epsilon^u])(\xi^\eta)^-\big)_{j+\frac{1}{2}} + \big((\{\epsilon^u\}+\alpha[\epsilon^u])(\xi^\eta)^+\big)_{j-\frac{1}{2}}\Big)dt \\
&+ \Big(\int_{I_j}\xi^\eta\xi^u_x dx - \big((\{\xi^\eta\}-\alpha[\xi^\eta])(\xi^u)^-\big)_{j+\frac{1}{2}} + \big((\{\xi^\eta\}-\alpha[\xi^\eta])(\xi^u)^+\big)_{j-\frac{1}{2}}\Big)dt \\
&- \Big(\int_{I_j}\epsilon^\eta\xi^u_x dx - \big((\{\epsilon^\eta\}-\alpha[\epsilon^\eta])(\xi^u)^-\big)_{j+\frac{1}{2}} + \big((\{\epsilon^\eta\}-\alpha[\epsilon^\eta])(\xi^u)^+\big)_{j-\frac{1}{2}}\Big)dt \\
&= \int_{I_j}(d\epsilon^\eta\xi^\eta + d\epsilon^u\xi^u)dx + \Big(\widetilde{\Theta}_{j-\frac{1}{2}} - \widetilde{\Theta}_{j+\frac{1}{2}}\Big)dt,
\end{aligned} \tag{2.26}$$

where $\widetilde{\Theta} = \big(\frac{1}{2}+\alpha\big)(\xi^u)^+(\xi^\eta)^- + \big(\frac{1}{2}-\alpha\big)(\xi^\eta)^+(\xi^u)^-$. The last equality follows from the definition of Radua projection $\mathcal{P}^{\pm\alpha}$ which leads to (for the error term $\epsilon^\eta = \mathcal{P}^{-\alpha}\eta - \eta$, $\epsilon^u = \mathcal{P}^\alpha u - u$)

$$\int_{I_j}\epsilon^u\xi^\eta_x dx = \int_{I_j}\epsilon^\eta\xi^u_x dx = (\{\epsilon^u\}+\alpha[\epsilon^u])_{j\pm\frac{1}{2}} = (\{\epsilon^\eta\}-\alpha[\epsilon^\eta])_{j\pm\frac{1}{2}} = 0,$$

and an integration by parts which leads to

$$\int_{I_j} \xi^u \xi_x^\eta dx + \int_{I_j} \xi^\eta \xi_x^u dx - \left((\{\xi^u\} + \alpha[\xi^u])(\xi^\eta)^-\right)_{j+\frac{1}{2}} + \left((\{\xi^u\} + \alpha[\xi^u])(\xi^\eta)^+\right)_{j-\frac{1}{2}}$$
$$- \left((\{\xi^\eta\} - \alpha[\xi^\eta])(\xi^u)^-\right)_{j+\frac{1}{2}} + \left((\{\xi^\eta\} - \alpha[\xi^\eta])(\xi^u)^+\right)_{j-\frac{1}{2}}$$
$$= \widetilde{\Theta}_{j-\frac{1}{2}} - \widetilde{\Theta}_{j+\frac{1}{2}}.$$

By Itô's lemma, we have

$$d(\xi^\eta)^2 = 2d\xi^\eta \xi^\eta + d\langle \xi^\eta, \xi^\eta \rangle_t,\ d(\xi^u)^2 = 2d\xi^u \xi^u + d\langle \xi^u, \xi^u \rangle_t. \tag{2.27}$$

Note that

$$d(\mathcal{P}^\alpha u) = \mathcal{P}^\alpha(du) = \mathcal{P}^\alpha(-\eta_x dt + \lambda_2 dW_t) = \mathcal{P}^\alpha(-\eta_x dt) + \lambda_2 \mathcal{P}^\alpha(dW_t).$$

For any test function $\widetilde{\varphi}$, we have

$$\int_{I_j} (d\mathcal{P}^\alpha u)\widetilde{\varphi} dx = \int_{I_j} \mathcal{P}^\alpha(-\eta_x)\widetilde{\varphi} dx dt + \int_{I_j} \lambda_2 \widetilde{\varphi} \mathcal{P}^\alpha(dW_t) dx. \tag{2.28}$$

Subtracting (2.3) from (2.28), we obtain

$$\int_{I_j} d\xi^u \widetilde{\varphi} dx = \Big(\int_{I_j} (-\eta_h \widetilde{\varphi}_x + \mathcal{P}^\alpha(-\eta_x)\widetilde{\varphi}) dx + (\breve{\eta}_h \widetilde{\varphi}^-)_{j+\frac{1}{2}} - (\breve{\eta}_h \widetilde{\varphi}^+)_{j-\frac{1}{2}} \Big) dt + \lambda_2 \int_{I_j} (\mathcal{P}^\alpha(dW_t) - dW_t)\widetilde{\varphi} dx.$$

Let us denote $\xi^u = \sum_{j=0}^k (\xi^u)_j^l \phi_j^l$. Following the exact same derivation of (2.16) in the proof of Theorem 2.2, we have

$$\int_{I_j} d\langle \xi^u, \xi^u \rangle_t dx = \lambda_2^2 \sum_{l=0}^k \mu_j^l \sum_m \Big(\int_{I_j} \phi_j^l \sqrt{\gamma_m} (\mathcal{P}^\alpha e_m(x) - e_m(x)) dx \Big)^2 dt$$
$$= \lambda_2^2 \mu_j^k \sum_m \Big(\int_{I_j} b_k x^k \sqrt{\gamma_m} (\mathcal{P}^\alpha e_m(x) - e_m(x)) dx \Big)^2 dt \le C \sum_m \gamma_m \int_{I_j} (\mathcal{P}^\alpha e_m(x) - e_m(x))^2 dx dt, \tag{2.29}$$

where the second equality follows from the definition of the generalized Radau projection (2.21) and $b_k x^k$ is the leading order term of the basis ϕ_j^l. In the same fashion, we have

$$\int_{I_j} d\langle \xi^\eta, \xi^\eta \rangle_t dx \le C \sum_m \gamma_m \int_{I_j} (\mathcal{P}^{-\alpha} e_m(x) - e_m(x))^2 dx dt. \tag{2.30}$$

The combination of (2.26)-(2.27) with (2.29)-(2.30) leads to

$$\begin{aligned} &\frac{1}{2} \int_{I_j} \left(d(\xi^\eta)^2 + d(\xi^u)^2 \right) dx \\ &= \int_{I_j} (d\epsilon^\eta \xi^\eta + d\epsilon^u \xi^u) dx + \left(\widetilde{\Theta}_{j-\frac{1}{2}} - \widetilde{\Theta}_{j+\frac{1}{2}} \right) dt + \frac{1}{2} \int_{I_j} \left(d\langle \xi^\eta, \xi^\eta \rangle_t + d\langle \xi^u, \xi^u \rangle_t \right) dx \\ &\le \int_{I_j} (d\epsilon^\eta \xi^\eta + d\epsilon^u \xi^u) dx + \left(\widetilde{\Theta}_{j-\frac{1}{2}} - \widetilde{\Theta}_{j+\frac{1}{2}} \right) dt + C \sum_m \gamma_m \int_{I_j} (\mathcal{P}^{\pm\alpha} e_m(x) - e_m(x))^2 dx dt. \end{aligned} \tag{2.31}$$

Summing over I_j and utilizing the periodic boundary conditions yield

$$\frac{1}{2} \int_I \left(d(\xi^\eta)^2 + d(\xi^u)^2 \right) dx \le \int_I (d\epsilon^\eta \xi^\eta + d\epsilon^u \xi^u) dx + C \sum_m \gamma_m \| \mathcal{P}^{\pm\alpha} e_m(x) - e_m(x) \|^2 dt. \tag{2.32}$$

By integrating (2.32) from 0 to t and noting that $\|\xi^\eta(x,0)\|^2 = \|\xi^u(x,0)\|^2 = 0$, we have

$$\|\xi^{\eta}(x,t)\|^2+\|\xi^{u}(x,t)\|^2 \le 2\Big(\int_0^t\int_I (d\epsilon^{\eta}\xi^{\eta}+d\epsilon^{u}\xi^{u})dxds\Big)+Ct\sum_m \gamma_m\|\mathcal{P}^{\pm\alpha}e_m(x)-e_m(x)\|^2$$
$$\le \Big(\int_0^t \|\xi^{\eta}(x,s)\|^2+\|\xi^{u}(x,s)\|^2 ds\Big)+Ch^{2k+2}+C\sum_m \gamma_m\|e_m\|^2_{H^{k+1}}h^{2k+2},$$

where the projection error is used in the last inequality. Applying the Gronwall's inequality and combining with the optimal projection error yields the desired optimal error estimate (2.22). □

Remark 2.2. We assumed sufficient regularity of the exact solutions to study the "best" convergence rate of the proposed numerical method, which has also been observed on some numerical examples in Section 5. In the literature [1,4,10], H^2 regularity for solutions to stochastic Maxwell equations has been assumed. In [3,4], the authors showed that for any given integer k, the solution is uniformly bounded in $\mathcal{D}(M^k)$ norm if u_0 has bounded $\mathcal{D}(M^k)$ norm, where $\|u\|_{\mathcal{D}(M^k)}=(\|u\|^2+\|M^k u\|^2)^{\frac{1}{2}}$ with the operator M defined by

$$M=\begin{pmatrix} 0 & \nabla\times \\ -\nabla\times & 0 \end{pmatrix}.$$

2.3. Multi-symplectic structure

The stochastic Maxwell equations (2.1) have a multi-symplectic structure, and we will show that the proposed DG method (2.2)-(2.3) preserves the multi-symplecticity.

Following the idea in [11], we introduce new variables

$$dv=udt,\ \ d\zeta=\eta dt,\ \ P=u+\frac{1}{2}\zeta_x,\ \ Q=\eta+\frac{1}{2}v_x,$$

and rewrite (2.1) into the following system:

$$\begin{cases} \frac{1}{2}\zeta_x=P-u, \\ \frac{1}{2}v_x=Q-\eta, \\ -dP-\frac{1}{2}\eta_x dt=-\lambda_2 dW_t, \\ -dQ-\frac{1}{2}u_x dt=\lambda_1 dW_t, \\ dv=udt, \\ d\zeta=\eta dt. \end{cases} \tag{2.33}$$

Introduce the notation $z=(u,\ \eta,\ v,\ \zeta,\ P,\ Q)^T$, and the system (2.33) can be rewritten as the multi-symplectic system

$$Mdz+Kz_x dt=\nabla_z S_1(z)dt+\nabla_z S_2(z)dW_t, \tag{2.34}$$

where

$$M=\begin{pmatrix} 0&0&0&0&0&0\\ 0&0&0&0&0&0\\ 0&0&0&0&-1&0\\ 0&0&0&0&0&-1\\ 0&0&1&0&0&0\\ 0&0&0&1&0&0 \end{pmatrix},\qquad K=\begin{pmatrix} 0&0&0&\frac{1}{2}&0&0\\ 0&0&\frac{1}{2}&0&0&0\\ 0&-\frac{1}{2}&0&0&0&0\\ -\frac{1}{2}&0&0&0&0&0\\ 0&0&0&0&0&0\\ 0&0&0&0&0&0 \end{pmatrix},$$

and

$$S_1(z)=Pu+Q\eta-\frac{u^2}{2}-\frac{\eta^2}{2},\qquad S_2(z)=\lambda_1\zeta-\lambda_2 v.$$

Applying the exterior derivative to the system (2.34) yields the following variation equation for the one-form Z:

$$MdZ+KZ_x dt=\nabla^2 S_1(z)Zdt. \tag{2.35}$$

Let $U,V\in\mathbb{R}^d$ be any solutions to the variation equation (2.35), and define

$$\omega(U,V)=MU\cdot V,\qquad \kappa(U,V)=KU\cdot V,$$

then the system (2.34) can be shown to satisfy the multi-symplectic conservation law given by

$$d\omega + \kappa_x dt = 0. \tag{2.36}$$

Multi-symplectic numerical method refers to the method that satisfies a consistent discrete version of this conservation law.

Since the new system (2.33) is equivalent to the original model (2.1), we can rewrite the proposed DG methods (2.2) and (2.3) into a consistent formulation for the system (2.33). We start by defining the variables v_h and ζ_h as follows: for u_h and η_h defined in (2.2) and (2.3), find $v_h,\ \zeta_h \in V_h^k$, such that for all test functions $\psi, \widetilde{\psi} \in V_h^k$, it holds that

$$\int_{I_j} dv_h \psi dx = \int_{I_j} u_h \psi dx dt, \qquad \int_{I_j} d\zeta_h \widetilde{\psi} dx = \int_{I_j} \eta_h \widetilde{\psi} dx dt, \tag{2.37}$$

which leads to the fact that $dv_h = u_h dt,\ d\zeta_h = \eta_h dt$. Next, find $P_h,\ Q_h \in V_h^k$, such that for all $\varphi, \widetilde{\varphi} \in V_h^k$, it holds that

$$\int_{I_j} (P_h - u_h)\varphi dx = -\frac{1}{2}\Big(\int_{I_j} \zeta_h \varphi_x dx - (\widehat{\zeta}_h \varphi^-)_{j+\frac{1}{2}} + (\widehat{\zeta}_h \varphi^+)_{j-\frac{1}{2}} \Big), \tag{2.38}$$

$$\int_{I_j} (Q_h - \eta_h)\widetilde{\varphi} dx = -\frac{1}{2}\Big(\int_{I_j} v_h \widetilde{\varphi}_x dx - (\widehat{v}_h \widetilde{\varphi}^-)_{j+\frac{1}{2}} + (\widehat{v}_h \widetilde{\varphi}^+)_{j-\frac{1}{2}} \Big), \tag{2.39}$$

where $\widehat{v}_h = \{v_h\} + 2n[v_h],\ \widehat{\zeta}_h = \{\zeta_h\} + 2m[\zeta_h]$ for some $m,\ n \in \mathbb{R}$ with $n - m = \alpha$ (for instance, $n = \alpha/2$ and $m = -\alpha/2$). By combining the derivative of (2.38) and (2.39) with the equations (2.3) and (2.2), and utilizing the fact that $dv_h = u_h dt,\ d\zeta_h = \eta_h dt$, we obtain

$$\int_{I_j} dP_h \phi dx = \frac{1}{2}\Big(\int_{I_j} \eta_h \phi_x dx - (\widehat{\eta}_h \phi^-)_{j+\frac{1}{2}} + (\widehat{\eta}_h \phi^+)_{j-\frac{1}{2}} \Big) dt + \int_{I_j} \lambda_2 \phi dW_t dx, \tag{2.40}$$

$$\int_{I_j} dQ_h \widetilde{\phi} dx = \frac{1}{2}\Big(\int_{I_j} u_h \widetilde{\phi}_x dx - (\widehat{u}_h \widetilde{\phi}^-)_{j+\frac{1}{2}} + (\widehat{u}_h \widetilde{\phi}^+)_{j-\frac{1}{2}} \Big) dt - \int_{I_j} \lambda_1 \widetilde{\phi} dW_t dx, \tag{2.41}$$

where $\widehat{u}_h = \{u_h\} - 2m[u_h],\ \widehat{\eta}_h = \{\eta_h\} - 2n[\eta_h]$. Combining (2.37)-(2.41), we have derived the following expression: find $P_h,\ Q_h,\ u_h,\ \eta_h,\ v_h,\ \zeta_h \in V_h^k$ such that

$$\begin{aligned}
&\int_{I_j} (P_h - u_h)\varphi dx = -\frac{1}{2}\Big(\int_{I_j} \zeta_h \varphi_x dx - (\widehat{\zeta}_h \varphi^-)_{j+\frac{1}{2}} + (\widehat{\zeta}_h \varphi^+)_{j-\frac{1}{2}} \Big),\\
&\int_{I_j} (Q_h - \eta_h)\widetilde{\varphi} dx = -\frac{1}{2}\Big(\int_{I_j} v_h \widetilde{\varphi}_x dx - (\widehat{v}_h \widetilde{\varphi}^-)_{j+\frac{1}{2}} + (\widehat{v}_h \widetilde{\varphi}^+)_{j-\frac{1}{2}} \Big),\\
&\int_{I_j} dP_h \phi dx = \frac{1}{2}\Big(\int_{I_j} \eta_h \phi_x dx - (\widehat{\eta}_h \phi^-)_{j+\frac{1}{2}} + (\widehat{\eta}_h \phi^+)_{j-\frac{1}{2}} \Big) dt + \int_{I_j} \lambda_2 \phi dW_t dx,\\
&\int_{I_j} dQ_h \widetilde{\phi} dx = \frac{1}{2}\Big(\int_{I_j} u_h \widetilde{\phi}_x dx - (\widehat{u}_h \widetilde{\phi}^-)_{j+\frac{1}{2}} + (\widehat{u}_h \widetilde{\phi}^+)_{j-\frac{1}{2}} \Big) dt - \int_{I_j} \lambda_1 \widetilde{\phi} dW_t dx,\\
&\int_{I_j} dv_h \psi dx = \int_{I_j} u_h \psi dx dt,\\
&\int_{I_j} d\zeta_h \widetilde{\psi} = \int_{I_j} \eta_h \widetilde{\psi} dx dt,
\end{aligned} \tag{2.42}$$

hold for any $\varphi,\ \widetilde{\varphi},\ \phi,\ \widetilde{\phi},\ \psi,\ \widetilde{\psi} \in V_h^k$. The numerical fluxes take the form

$$\widehat{u}_h = \{u_h\} - 2m[u_h],\ \ \widehat{\eta}_h = \{\eta_h\} - 2n[\eta_h],\ \ \widehat{v}_h = \{v_h\} + 2n[v_h],\ \ \widehat{\zeta}_h = \{\zeta_h\} + 2m[\zeta_h].$$

Note that the method (2.42) can be rewritten into the corresponding DG scheme for the new system (2.34): find $z_h \in (V_h^k)^6$, such that for all $\boldsymbol{\varphi} \in (V_h^k)^6$, it holds that

$$\int_{I_j} M dz_h \cdot \boldsymbol{\varphi} dx - \Big(\int_{I_j} K z_h \cdot \boldsymbol{\varphi}_x dx - \big(\widehat{K z_h} \cdot \boldsymbol{\varphi}^-\big)_{j+\frac{1}{2}} + \big(\widehat{K z_h} \cdot \boldsymbol{\varphi}^+\big)_{j-\frac{1}{2}} \Big) dt$$
$$= \int_{I_j} \nabla S_1(z_h) \cdot \boldsymbol{\varphi} dx dt + \int_{I_j} \nabla S_2(z_h) \cdot \boldsymbol{\varphi} dW_t dx, \tag{2.43}$$

where $\widehat{K z_h}$ is the numerical flux in the form

$$\widehat{K z_h} = K\{z_h\} + A[z_h], \qquad A = \begin{pmatrix} 0 & 0 & 0 & m & 0 & 0 \\ 0 & 0 & n & 0 & 0 & 0 \\ 0 & n & 0 & 0 & 0 & 0 \\ m & 0 & 0 & 0 & 0 & 0 \\ 0 & 0 & 0 & 0 & 0 & 0 \\ 0 & 0 & 0 & 0 & 0 & 0 \end{pmatrix}.$$

Applying the exterior derivative to this scheme (2.43) leads to the variational equation

$$\int_{I_j} M dZ_h \cdot \varphi dx - \Big(\int_{I_j} K Z_h \cdot \varphi_x dx - \big(\widehat{K Z_h} \cdot \varphi^-\big)_{j+\frac{1}{2}} + \big(\widehat{K Z_h} \cdot \varphi^+\big)_{j-\frac{1}{2}} \Big) dt = \int_{I_j} \nabla^2 S_1(z) Z_h \cdot \varphi dx dt. \tag{2.44}$$

Following the proof of multi-symplecticity of DG methods in [24], we have the following results.

Lemma 2.2. *For any $U_h, V_h \in V_h^k$, we have*

$$K U_h^- \cdot V_h^- - \widehat{K U_h} \cdot V_h^- + \widehat{K V_h} \cdot U_h^- = K U_h^+ \cdot V_h^+ - \widehat{K U_h} \cdot V_h^+ + \widehat{K V_h} \cdot U_h^+ = \mathcal{F}_K(U_h, V_h), \tag{2.45}$$

where

$$\mathcal{F}_K(U_h, V_h) = \{K U_h \cdot V_h\} - \widehat{K U_h} \cdot \{V_h\} + \widehat{K V_h} \cdot \{U_h\}.$$

Theorem 2.4 (***Conservation of multi-symplecticity***). *Let U_h, V_h be any solutions to the variational equation (2.44), we have the semi-discrete version of the multi-symplectic conservation laws*

$$\int_{I_j} d(M U_h \cdot V_h) dx - \Big(\mathcal{F}_K(U_h, V_h)_{j+\frac{1}{2}} - \mathcal{F}_K(U_h, V_h)_{j-\frac{1}{2}} \Big) dt = 0. \tag{2.46}$$

Proof. By Itô's lemma, we have

$$d(M U_h \cdot V_h) = M dU_h \cdot V_h + M U_h \cdot dV_h + M d\langle U_h, V_h \rangle_t. \tag{2.47}$$

Note that $U_h(\omega, x, t), V_h(\omega, x, t) \in V_h^k$, which can be rewritten as

$$U_h(\omega, x, t)\big|_{I_j} = \sum_{l=0}^{k} \varphi_j^l(x) U_j^l(\omega, t), \qquad V_h(\omega, x, t)\big|_{I_j} = \sum_{l=0}^{k} \varphi_j^l(x) V_j^l(\omega, t),$$

where $\{\varphi_j^l(x),\ l = 0, \cdots, k\}$ is a set of basis. Therefore one has

$$dU_h = \sum_{l=0}^{k} \varphi_j^l(x) dU_j^l, \qquad dV_h = \sum_{l=0}^{k} \varphi_j^l(x) dV_j^l.$$

In the variational equation (2.44), we set dZ_h to be dU_h, and take the test function φ to be dV_h. As the second and third terms in (2.44) are both drift terms, we can conclude that $\int_{I_j} M d\langle U_h, V_h \rangle_t dx = 0$. By combining (2.47) and (2.44), and utilizing the fact that M is anti-symmetric and $\nabla^2 S_1$ is symmetric, we obtain

$$\int_{I_j} d(M U_h \cdot V_h) dx = \int_{I_j} (M dU_h \cdot V_h + M U_h \cdot dV_h) dx = \int_{I_j} (M dU_h \cdot V_h - M dV_h \cdot U_h) dx$$
$$= \Big(\int_{I_j} K U_h \cdot (V_h)_x dx - \big(\widehat{K U_h} \cdot V_h^-\big)_{j+\frac{1}{2}} + \big(\widehat{K U_h} \cdot V_h^+\big)_{j-\frac{1}{2}} \Big) dt + \int_{I_j} \nabla^2 S_1 U_h \cdot V_h dx dt$$

$$
\begin{aligned}
&-\left(\int_{I_j} KV_h\cdot(U_h)_x dx-\left(\widehat{KV_h}\cdot U_h^-\right)_{j+\frac{1}{2}}+\left(\widehat{KV_h}\cdot U_h^+\right)_{j-\frac{1}{2}}\right)dt-\int_{I_j}\nabla^2 S_1 V_h\cdot U_h dxdt\\
&=\left(\left(KU_h^-\cdot V_h^- -\widehat{KU_h}\cdot V_h^-+\widehat{KV_h}\cdot U_h^-\right)_{j+\frac{1}{2}}-\left(KU_h^+\cdot V_h^+-\widehat{KU_h}\cdot V_h^++\widehat{KV_h}\cdot U_h^+\right)_{j-\frac{1}{2}}\right)dt\\
&=\left(\mathcal{F}_K(U_h,V_h)_{j+\frac{1}{2}}-\mathcal{F}_K(U_h,V_h)_{j-\frac{1}{2}}\right)dt,
\end{aligned}
$$

where the last equality follows from Lemma 2.2. This finishes the proof. □

3. Two-dimensional stochastic Maxwell equations with additive noise

In this section, we will present the discontinuous Galerkin methods for two-dimensional stochastic Maxwell equations with additive noise with periodic boundary conditions on cartesian meshes, and study the stability, error estimate and multi-symplecticity of the proposed methods.

The two-dimensional rectangular computational domain is set to be $I\times J$, and we consider the rectangular partition with the cells denoted by $I_i\times J_j=[x_{i-\frac{1}{2}},x_{i+\frac{1}{2}}]\times[y_{j-\frac{1}{2}},y_{j+\frac{1}{2}}]$ for $i=1,2,\cdots,N_x$ and $j=1,2\cdots,N_y$. Let $x_i=\frac{1}{2}(x_{i-\frac{1}{2}}+x_{i+\frac{1}{2}})$, and $y_j=\frac{1}{2}(y_{j-\frac{1}{2}}+y_{j+\frac{1}{2}})$. Furthermore, we define the mesh size in both directions as $h_{x,i}=x_{i+\frac{1}{2}}-x_{i-\frac{1}{2}}$, $h_{y,j}=y_{j+\frac{1}{2}}-y_{j-\frac{1}{2}}$, with $h_x=\max_i h_{x,i}$, $h_y=\max_j h_{y,j}$ and $h=\max(h_x,h_y)$ being the maximum mesh size. Similar to the one-dimensional case, we define the two dimensional piecewise polynomial space $\mathbb{V}_h^k$ as follows:

$$
\mathbb{V}_h^k=\{v(x,y):v|_{I_i\times J_j}\in Q^k(I_i\times J_j)=P^k(I_i)\otimes P^k(J_j),\ \ i=1,2,\cdots,N_x;\ j=1,2,\cdots,N_y\}.
$$

The two-dimensional stochastic Maxwell equations with additive noise take the form

$$
\begin{cases}
-dE+T_x dt-S_y dt=\lambda_1 dW_t,\\
dS+E_y dt=\lambda_2 dW_t,\\
dT-E_x dt=\lambda_2 dW_t.
\end{cases}
\tag{3.1}
$$

The DG scheme for (3.1) is formulated as follows: find $E_h,\ S_h,\ T_h\in\mathbb{V}_h^k$, such that for all test functions $\varphi,\ \psi,\ \phi\in\mathbb{V}_h^k$, it holds that

$$
\begin{aligned}
\int_{J_j}\int_{I_i} dE_h\varphi dxdy=&-\int_{J_j}\left(\int_{I_i} T_h\varphi_x dx-\left(\widetilde{(T_h)_{\alpha_1}}\varphi^-\right)_{i+\frac{1}{2},y}+\left(\widetilde{(T_h)_{\alpha_1}}\varphi^+\right)_{i-\frac{1}{2},y}\right)dydt\\
&+\int_{I_i}\left(\int_{J_j} S_h\varphi_y dy-\left(\widetilde{(S_h)_{-\alpha_2}}\varphi^-\right)_{x,j+\frac{1}{2}}+\left(\widetilde{(S_h)_{-\alpha_2}}\varphi^+\right)_{x,j-\frac{1}{2}}\right)dxdt\\
&-\int_{J_j}\int_{I_i}\lambda_1\varphi dW_t dxdy,
\end{aligned}
\tag{3.2}
$$

$$
\begin{aligned}
\int_{J_j}\int_{I_i} dS_h\psi dxdy=&\int_{I_i}\left(\int_{J_j} E_h\psi_y dy-\left(\widetilde{(E_h)_{\alpha_2}}\psi^-\right)_{x,j+\frac{1}{2}}+\left(\widetilde{(E_h)_{\alpha_2}}\psi^+\right)_{x,j-\frac{1}{2}}\right)dxdt\\
&+\int_{J_j}\int_{I_i}\lambda_2\psi dW_t dxdy,
\end{aligned}
\tag{3.3}
$$

$$
\begin{aligned}
\int_{J_j}\int_{I_i} dT_h\phi dxdy=&-\int_{J_j}\left(\int_{I_i} E_h\phi_x dx-\left(\widetilde{(E_h)_{-\alpha_1}}\phi^-\right)_{i+\frac{1}{2},y}+\left(\widetilde{(E_h)_{-\alpha_1}}\phi^+\right)_{i-\frac{1}{2},y}\right)dydt\\
&+\int_{J_j}\int_{I_i}\lambda_2\phi dW_t dxdy,
\end{aligned}
\tag{3.4}
$$

where the generalized alternating numerical fluxes are defined as follows:

$$
\widetilde{g_\alpha}=\{g\}+\alpha[g],\qquad \text{for } g\in\mathbb{V}_h^k \text{ and } \alpha\in\{\pm\alpha_1,\pm\alpha_2\}\subset\mathbb{R}.
$$

For the ease of presentation, we also introduce the following operators: for $\alpha\in\mathbb{R}$, $f,\ g\in\mathbb{V}_h^k$,

$$\mathcal{A}_{I_i}(f,g;\alpha)=\int_{I_i} fg_x dx-(\widetilde{f_\alpha}g^-)_{i+\frac{1}{2},y}+(\widetilde{f_\alpha}g^+)_{i-\frac{1}{2},y},$$

$$\mathcal{A}_{J_j}(f,g;\alpha)=\int_{J_j} fg_y dy-(\widetilde{f_\alpha}g^-)_{x,j+\frac{1}{2}}+(\widetilde{f_\alpha}g^+)_{x,j-\frac{1}{2}}.$$

3.1. Semi-discrete energy law

Similar to the 1D case, we start by presenting the linear energy growth property of the exact solutions. In [2,11] the authors provided continuous energy law in $\mathbb{R}^3$, which has the following form in $\mathbb{R}^2$:

Theorem 3.1 (***Continuous energy law***). *Let $E,\ S,\ T$ be the solutions to the equation (3.1) under the periodic boundary condition, and define the two-dimensional energy as $\mathcal{E}(t)=\int_J\int_I E(x,y,t)^2+S(x,y,t)^2+T(x,y,t)^2dxdy$, then for any t, the global stochastic energy satisfies the following energy law*

$$\mathcal{E}(t)=\mathcal{E}(0)+2\int_0^t\int_J\int_I \lambda_2(S+T)-\lambda_1 E dW_s dxdy+(\lambda_1^2+2\lambda_2^2)Tr(\mathcal{Q})t, \tag{3.5}$$

and, after taking the expectation,

$$\mathbb{E}\Big(\mathcal{E}(t)\Big)=\mathcal{E}(0)+(\lambda_1^2+2\lambda_2^2)Tr(\mathcal{Q})t. \tag{3.6}$$

The proof is skipped here as it follows the same analysis as that of Theorem 2.1.

Theorem 3.2 (***Semi-discrete energy law***). *Let $E_h(\omega,x,y,t)$, $S_h(\omega,x,y,t)$ and $T_h(\omega,x,y,t)$ be the numerical solutions to the DG methods (3.2) - (3.4).*
(a): For any $t\in[0,T]$, the numerical solutions satisfy the semi-discrete energy law

$$\begin{aligned}&\|E_h(\omega,x,y,t)\|^2+\|S_h(\omega,x,y,t)\|^2+\|T_h(\omega,x,y,t)\|^2 \\ &=2\int_0^t\int_J\int_I \lambda_2(T_h+S_h)-\lambda_1 E_h dW_s dxdy+\|E_h(x,y,0)\|^2+\|S_h(x,y,0)\|^2+\|T_h(x,y,0)\|^2+(\lambda_1^2+2\lambda_2^2)Kt,\end{aligned} \tag{3.7}$$

and

$$\begin{aligned}&\mathbb{E}\Big(\|E_h(x,y,t)\|^2+\|S_h(x,y,t)\|^2+\|T_h(x,y,t)\|^2\Big) \\ &\qquad=\|E_h(x,y,0)\|^2+\|S_h(x,y,0)\|^2+\|T_h(x,y,0)\|^2+(\lambda_1^2+2\lambda_2^2)Kt,\end{aligned} \tag{3.8}$$

with

$$K=\sum_{i,j}\sum_{l=0}^{k^2+2k}\mu_{i,j}^l\sum_{m=1}^{\infty}\Big(\int_{J_j}\int_{I_i}\phi_{i,j}^l\sqrt{\gamma_m}e_m dxdy\Big)^2, \tag{3.9}$$

where $\{\phi_{i,j}^l, i,j=0,\cdots,k\}$ represents the set of Legendre basis over cell $J_j\times I_i$, and $\mu_{i,j}^l=(\int_{J_j}\int_{I_i}(\phi_{i,j}^l)^2dxdy)^{-1}$.
(b) The constant K is bounded by $(k^2+2k)Tr(\mathcal{Q})$ with k being the polynomial degree of the DG methods. Moreover, if there exists some constant $\nu\in(0,2)$ such that the series $\sum_{m=1}^{\infty}\gamma_m(K_m)^\nu<\infty$ with $K_m=\|\nabla e_m\|_\infty$, we can show that $K=Tr(\mathcal{Q})+O(h^\nu)$, i.e., K is an approximation of $Tr(\mathcal{Q})$ appearing in the continuous energy law (3.5)-(3.6).

Proof. (a): By Itô's lemma, we know that

$$d(E_h)^2=2E_h dE_h+d\langle E_h,E_h\rangle_t,\ \ d(S_h)^2=2S_h dS_h+d\langle S_h,S_h\rangle_t,\ \ d(T_h)^2=2T_h dT_h+d\langle T_h,T_h\rangle_t. \tag{3.10}$$

By taking the test functions $\varphi=E_h$, $\psi=S_h$ and $\phi=T_h$ in (3.2)-(3.4), and adding these equations, we have

$$\int_{J_j}\int_{I_i}(dE_h)E_h+(dS_h)S_h+(dT_h)T_h dxdy$$
$$=\int_{J_j}-(\Theta)_{i-\frac{1}{2},y}+(\Theta)_{i+\frac{1}{2},y}dydt+\int_{I_i}(\widetilde{\Theta})_{x,j-\frac{1}{2}}-(\widetilde{\Theta})_{x,j+\frac{1}{2}}dxdt$$
$$+\int_{J_j}\int_{I_i}\lambda_2(T_h+S_h)-\lambda_1 E_h dW_t dxdy, \tag{3.11}$$

where

$$\Theta=\big(\frac{1}{2}+\alpha_1\big)T_h^+E_h^-+\big(\frac{1}{2}-\alpha_1\big)E_h^+T_h^-,\ \ \widetilde{\Theta}=\big(\frac{1}{2}+\alpha_2\big)E_h^+S_h^-+\big(\frac{1}{2}-\alpha_2\big)E_h^-S_h^+.$$

Following the same analysis as in Theorem 2.2 (more specifically, the derivation of Eq. (2.16)), we can evaluate the terms and have

$$\int_{J_j}\int_{I_i}d\langle S_h,S_h\rangle_t dxdy=\int_{J_j}\int_{I_i}d\langle T_h,T_h\rangle_t dxdy=\lambda_2^2\sum_{l=0}^{k^2+2k}\mu_{i,j}^l\sum_{m=1}^{\infty}\Big(\int_{J_j}\int_{I_i}\phi_{i,j}^l\sqrt{\gamma_m}e_m dxdy\Big)^2dt,$$
$$\int_{J_j}\int_{I_i}d\langle E_h,E_h\rangle_t dxdy=\lambda_1^2\sum_{l=0}^{k^2+2k}\mu_{i,j}^l\sum_{m=1}^{\infty}\Big(\int_{J_j}\int_{I_i}\phi_{i,j}^l\sqrt{\gamma_m}e_m dxdy\Big)^2dt. \tag{3.12}$$

By combining the equations (3.10)-(3.12), summing over all the cells and integrating in time from 0 to t, we can obtain

$$\|E_h(x,y,t)\|^2+\|S_h(x,y,t)\|^2+\|T_h(x,y,t)\|^2 \tag{3.13}$$
$$=2\int_0^t\int_J\int_I\lambda_2(T_h+S_h)-\lambda_1E_hdW_sdxdy+\|E_h(x,y,0)\|^2+\|S_h(x,y,0)\|^2+\|T_h(x,y,0)\|^2+(\lambda_1^2+2\lambda_2^2)Kt.$$

Note that $\mathbb{E}\Big(\int_0^t\int_J\int_I\lambda_2(T_h+S_h)-\lambda_1E_hdW_sdxdy\Big)=0$ since it is an Itô integral, therefore taking expectation of (3.13) leads to the semi-discrete energy law (3.8).

(b): The estimate of the constant K follows an exact same analysis as in the proof of Theorem 2.2 (b), that is,

$$K\le(k^2+2k)Tr(\mathcal{Q}),$$

and if $\sum_{m=1}^{\infty}\gamma_m(K_m)^\nu<\infty$, we can show that

$$K-Tr(\mathcal{Q})=O(h^\nu).$$

If W_t is the standard Brownian motion, it can be shown that $K=Tr(\mathcal{Q})$ (see Remark 2.1), which means that the two-dimensional continuous energy law (3.5) is exactly preserved by the proposed method. □

3.2. Optimal error estimate

In this section we study the convergence rate of the DG scheme (3.2)-(3.4). We start with defining the generalized Radau projection in $\mathbb{R}^2$ as

$$\mathbb{P}_x^\alpha=\mathcal{P}_x^\alpha\otimes\mathcal{P}_y,\ \mathbb{P}_y^\alpha=\mathcal{P}_x\otimes\mathcal{P}_y^\alpha,\ \mathbb{P}^{\alpha,\beta}=\mathcal{P}_x^\alpha\otimes\mathcal{P}_y^\beta, \tag{3.14}$$

where $\mathcal{P}$ is the L^2 projection, and $\mathcal{P}^\alpha$, $\mathcal{P}^\beta$ (with $\alpha,\beta\neq0$) are the generalized Radau projection defined in (2.21). The following lemmas are provided in [23] and will be useful in our analysis.

Lemma 3.1 (***Superconvergence property***). *For any smooth function $w\in H^{k+1}$, denote $\epsilon=\mathbb{P}^{\alpha,\beta}w-w$, with $\mathbb{P}^{\alpha,\beta}$ being the projection defined in (3.14). For any $v\in\mathbb{V}_h^k$, there exists some constant C such that*

$$\Big|\sum_{i,j}\int_{J_j}\mathcal{A}_{I_i}(\epsilon,v,\alpha)dy\Big|\le Ch^{k+1}\|v\|,\quad\Big|\sum_{i,j}\int_{I_i}\mathcal{A}_{J_j}(\epsilon,v,\alpha)dx\Big|\le Ch^{k+1}\|v\|.$$

Lemma 3.2 (***Projection error***). *Let Π be any projection defined in (3.14). For any smooth function $w(x, y) \in H^{k+1}$, there exists some constant C, such that*

$$\|\Pi w - w\| \leq Ch^{k+1}.$$

Now we turn to the main result on the error estimate of the DG methods.

Theorem 3.3 (***Optimal error estimate***). *Let $E_h, S_h, T_h \in \mathbb{V}_h^k$ be the numerical solutions given by the DG scheme (3.2) - (3.4), and $E, T, S \in L^2(\Omega \times [0, T]; H^{k+2})$ are strong solutions to (3.1). With the initial conditions chosen as*

$$E_h(x, y, 0) = \mathbb{P}^{-\alpha_1,\alpha_2} E(x, y, 0);\ S_h(x, y, 0) = \mathbb{P}_y^{-\alpha_2} S(x, y, 0);\ T_h(x, y, 0) = \mathbb{P}_x^{\alpha_1} T(x, y, 0),$$

and the assumption $\sum_m \gamma_m \|e_m\|^2_{H^{k+1}} < \infty$, there holds the following error estimates

$$\|E - E_h\|^2 + \|S - S_h\|^2 + \|T - T_h\|^2 \leq Ch^{2k+2}, \tag{3.15}$$

where the constant C denotes a generic positive constant independent of the spatial cell sizes h.

Proof. Since both the numerical and exact solutions satisfy the equations (3.2) - (3.4), we have the error equations

$$\int_{J_j}\int_{I_i} d(E - E_h)\varphi dxdy = -\int_{J_j} \mathcal{A}_{I_i}(T - T_h, \varphi; \alpha_1)dydt + \int_{I_i} \mathcal{A}_{J_j}(S - S_h, \varphi; -\alpha_2)dxdt, \tag{3.16}$$

$$\int_{J_j}\int_{I_i} d(S - S_h)\psi dxdy = \int_{I_i} \mathcal{A}_{J_j}(E - E_h, \psi; \alpha_2)dxdt, \tag{3.17}$$

$$\int_{J_j}\int_{I_i} d(T - T_h)\phi dxdy = -\int_{J_j} \mathcal{A}_{I_i}(E - E_h, \phi; -\alpha_1)dydt. \tag{3.18}$$

Let

$$\xi^E = \mathbb{P}^{-\alpha_1,\alpha_2} E - E_h, \quad \xi^S = \mathbb{P}_y^{-\alpha_2} S - S_h, \quad \xi^T = \mathbb{P}_x^{\alpha_1} T - T_h,$$
$$\epsilon^E = \mathbb{P}^{-\alpha_1,\alpha_2} E - E, \quad \epsilon^S = \mathbb{P}_y^{-\alpha_2} S - S, \quad \epsilon^T = \mathbb{P}_x^{\alpha_1} T - T,$$

which leads to the decomposition of the error into two terms as

$$E - E_h = \xi^E - \epsilon^E,\ \ S - S_h = \xi^S - \epsilon^S,\ \ T - T_h = \xi^T - \epsilon^T.$$

By choosing the test functions as $\varphi = \xi^E,\ \psi = \xi^S,\ \phi = \xi^T$ in (3.16)-(3.18), and noting that

$$\int_{J_j} \mathcal{A}_{I_i}(\epsilon^T, \xi^E; \alpha_1)dydt = \int_{I_i} \mathcal{A}_{J_j}(\epsilon^S, \xi^E; -\alpha_2)dxdt = 0$$

by the definition of the projections, we have

$$\int_{J_j}\int_{I_i} d\xi^E\xi^E - d\epsilon^E\xi^E dxdy = -\int_{J_j} \mathcal{A}_{I_i}(\xi^T, \xi^E; \alpha_1)dydt + \int_{I_i} \mathcal{A}_{J_j}(\xi^S, \xi^E; -\alpha_2)dxdt, \tag{3.19}$$

$$\int_{J_j}\int_{I_i} d\xi^S\xi^S - d\epsilon^S\xi^S dxdy = \int_{I_i} \mathcal{A}_{J_j}(\xi^E, \xi^S; \alpha_2)dxdt - \int_{I_i} \mathcal{A}_{J_j}(\epsilon^E, \xi^S; \alpha_2)dxdt, \tag{3.20}$$

$$\int_{J_j}\int_{I_i} d\xi^T\xi^T - d\epsilon^T\xi^T dxdy = -\int_{J_j} \mathcal{A}_{I_i}(\xi^E, \xi^T; -\alpha_1)dydt + \int_{J_j} \mathcal{A}_{I_i}(\epsilon^E, \xi^T; -\alpha_1)dydt. \tag{3.21}$$

Summing up (3.19)-(3.21) and using integration by parts, we obtain

$$\begin{aligned}
&\int_{J_j}\int_{I_i} d\xi^E\xi^E + d\xi^S\xi^S + d\xi^T\xi^T dxdy \\
&= \int_{J_j}\int_{I_i} d\epsilon^E\xi^E + d\epsilon^S\xi^S + d\epsilon^T\xi^T dxdy - \int_{J_j}\left(\Pi_{i-\frac{1}{2},y} - \Pi_{i+\frac{1}{2},y}\right)dydt + \int_{I_i}\left(\bar{\Pi}_{x,j-\frac{1}{2}} - \bar{\Pi}_{x,j+\frac{1}{2}}\right)dxdt \\
&\quad - \int_{I_i}\mathcal{A}_{J_j}(\epsilon^E,\xi^S;\alpha_2)dxdt + \int_{J_j}\mathcal{A}_{I_i}(\epsilon^E,\xi^T;-\alpha_1)dydt,
\end{aligned} \tag{3.22}$$

where

$$\Pi = \left(\frac{1}{2}+\alpha_1\right)(\xi^T)^+(\xi^E)^- + \left(\frac{1}{2}-\alpha_1\right)(\xi^T)^-(\xi^E)^+,\quad \bar{\Pi} = \left(\frac{1}{2}+\alpha_2\right)(\xi^S)^-(\xi^E)^+ + \left(\frac{1}{2}-\alpha_2\right)(\xi^S)^+(\xi^E)^-.$$

By Itô's lemma, we have

$$d(\xi^E)^2 = 2d\xi^E\xi^E + d\langle\xi^E,\xi^E\rangle_t,\quad d(\xi^S)^2 = 2d\xi^S\xi^S + d\langle\xi^S,\xi^S\rangle_t,\quad d(\xi^T)^2 = 2d\xi^T\xi^T + d\langle\xi^T,\xi^T\rangle_t.$$

Following the exact same analysis as shown in the proof of Theorem 2.3, we have

$$\begin{aligned}
&\int_{J_j}\int_{I_i} d\langle\xi^E,\xi^E\rangle_t dxdy \le C\sum_m \gamma_m \int_{J_j}\int_{I_i} (\mathbb{P}^{-\alpha_1,\alpha_2}(e_m(x,y)) - e_m(x,y))^2 dxdydt, \\
&\int_{J_j}\int_{I_i} d\langle\xi^S,\xi^S\rangle_t dxdy \le C\sum_m \gamma_m \int_{J_j}\int_{I_i} (\mathbb{P}_y^{-\alpha_2}(e_m(x,y)) - e_m(x,y))^2 dxdydt, \\
&\int_{J_j}\int_{I_i} d\langle\xi^T,\xi^T\rangle_t dxdy \le C\sum_m \gamma_m \int_{J_j}\int_{I_i} (\mathbb{P}_x^{\alpha_1}(e_m(x,y)) - e_m(x,y))^2 dxdydt.
\end{aligned}$$

Therefore, by summing over all the cells $I_i \times J_j$ in (3.22) and applying the superconvergence property in Lemma 3.1, we obtain

$$\begin{aligned}
&\frac{1}{2}\int_J\int_I d(\xi^E)^2 + d(\xi^S)^2 + (d\xi^T)^2 dxdy \\
&= \frac{1}{2}\int_J\int_I (d\langle\xi^E,\xi^E\rangle_t + d\langle\xi^S,\xi^S\rangle_t + d\langle\xi^T,\xi^T\rangle_t)dxdy + \int_J\int_I d\xi^E\xi^E + d\xi^S\xi^S + d\xi^T\xi^T dxdy \\
&\le \int_J\int_I d\epsilon^E\xi^E + d\epsilon^S\xi^S + d\epsilon^T\xi^T dxdy + Ch^{k+1}\left(\|\xi^T\| + \|\xi^S\|\right)dt \\
&\quad + C\sum_m \gamma_m\left(\|\mathbb{P}^{-\alpha_1,\alpha_2}(e_m) - e_m\|^2 + \|\mathbb{P}_x^{\alpha_1}(e_m) - e_m\|^2 + \|\mathbb{P}_y^{-\alpha_2}(e_m) - e_m\|^2\right)dt.
\end{aligned} \tag{3.23}$$

Integrating (3.23) over t, applying the projection error property and Young's inequality, we can show that

$$\|\xi^E\|^2 + \|\xi^S\|^2 + \|\xi^T\|^2 \le C\int_0^t \|\xi^E(x,y,s)\|^2 + \|\xi^S(x,y,s)\|^2 + \|\xi^T(x,y,s)\|^2 ds + Ch^{2k+2} + C\sum_m \gamma_m \|e_m\|_{H^{k+1}}^2 h^{2k+2}.$$

Applying the Gronwall's inequality and combining with the optimal projection error yields the desired optimal error estimate (3.15). □

3.3. Multi-symplectic structure

Similar to the 1D case, to rewrite the two-dimensional stochastic Maxwell equations (3.1) in the multi-symplectic form. Following the idea in [11], we introduce the new variables such that

$$du = Edt,\ dv = Sdt,\ dw = Tdt,\ P = T - \frac{1}{2}u_x,\ Q = S + \frac{1}{2}u_y,\ R = E - \frac{1}{2}w_x + \frac{1}{2}v_y,$$

and the system (3.1) becomes

$$\begin{cases} -\frac{1}{2}u_x = P - T, \\ \frac{1}{2}u_y = Q - S, \\ -\frac{1}{2}w_x + \frac{1}{2}v_y = R - E, \\ -dP + \frac{1}{2}E_x dt = -\lambda_2 dW_t, \\ -dQ - \frac{1}{2}E_y dt = -\lambda_2 dW_t, \\ -dR + \frac{1}{2}T_x dt - \frac{1}{2}S_y dt = \lambda_1 dW_t, \\ dw = T dt, \\ dv = S dt, \\ du = E dt. \end{cases} \tag{3.24}$$

We set $z = (T, S, E, w, v, u, P, Q, R)^T$, and define

$$M = \begin{pmatrix} 0 & 0 & 0 & 0 & 0 & 0 & 0 & 0 & 0 \\ 0 & 0 & 0 & 0 & 0 & 0 & 0 & 0 & 0 \\ 0 & 0 & 0 & 0 & 0 & 0 & 0 & 0 & 0 \\ 0 & 0 & 0 & 0 & 0 & 0 & -1 & 0 & 0 \\ 0 & 0 & 0 & 0 & 0 & 0 & 0 & -1 & 0 \\ 0 & 0 & 0 & 0 & 0 & 0 & 0 & 0 & -1 \\ 0 & 0 & 0 & 1 & 0 & 0 & 0 & 0 & 0 \\ 0 & 0 & 0 & 0 & 1 & 0 & 0 & 0 & 0 \\ 0 & 0 & 0 & 0 & 0 & 1 & 0 & 0 & 0 \end{pmatrix},$$

$$K_1 = \begin{pmatrix} 0 & 0 & 0 & 0 & 0 & -\frac{1}{2} & 0 & 0 & 0 \\ 0 & 0 & 0 & 0 & 0 & 0 & 0 & 0 & 0 \\ 0 & 0 & 0 & -\frac{1}{2} & 0 & 0 & 0 & 0 & 0 \\ 0 & 0 & \frac{1}{2} & 0 & 0 & 0 & 0 & 0 & 0 \\ 0 & 0 & 0 & 0 & 0 & 0 & 0 & 0 & 0 \\ \frac{1}{2} & 0 & 0 & 0 & 0 & 0 & 0 & 0 & 0 \\ 0 & 0 & 0 & 0 & 0 & 0 & 0 & 0 & 0 \\ 0 & 0 & 0 & 0 & 0 & 0 & 0 & 0 & 0 \\ 0 & 0 & 0 & 0 & 0 & 0 & 0 & 0 & 0 \end{pmatrix}, \quad K_2 = \begin{pmatrix} 0 & 0 & 0 & 0 & 0 & 0 & 0 & 0 & 0 \\ 0 & 0 & 0 & 0 & 0 & \frac{1}{2} & 0 & 0 & 0 \\ 0 & 0 & 0 & 0 & \frac{1}{2} & 0 & 0 & 0 & 0 \\ 0 & 0 & 0 & 0 & 0 & 0 & 0 & 0 & 0 \\ 0 & 0 & -\frac{1}{2} & 0 & 0 & 0 & 0 & 0 & 0 \\ 0 & -\frac{1}{2} & 0 & 0 & 0 & 0 & 0 & 0 & 0 \\ 0 & 0 & 0 & 0 & 0 & 0 & 0 & 0 & 0 \\ 0 & 0 & 0 & 0 & 0 & 0 & 0 & 0 & 0 \\ 0 & 0 & 0 & 0 & 0 & 0 & 0 & 0 & 0 \end{pmatrix},$$

$$S_1 = PT + QS + RE - \frac{T^2 + S^2 + E^2}{2}, \ S_2 = \lambda_1 u - \lambda_2 (w + v),$$

therefore, the two-dimensional stochastic Maxwell equations (3.1) can be rewritten in the following multi-symplectic system

$$M dz + K_1 z_x dt + K_2 z_y dt = \nabla S_1(z) dt + \nabla S_2(z) dW_t. \tag{3.25}$$

Its variational equation takes the form

$$M dZ + K_1 Z_x dt + K_2 Z_y dt = \nabla^2 S_1(z) Z dt. \tag{3.26}$$

Let $U,\ V$ be any solution to the variational equation (3.26), and define $\omega = MU \cdot V,\ \kappa_x = K_1 U \cdot V,\ \kappa_y = K_2 U \cdot V$, then we can derive the multi-symplectic conservation law given by

$$d\omega + \kappa_x dt + \kappa_y dt = 0.$$

Since the new system (3.24) is equivalent to the original model (3.1), we can rewrite the proposed DG methods (3.2)-(3.4) into a consistent formulation for the system (3.24). For $E_h,\ S_h,\ T_h$ defined in (3.2) - (3.4), find $w_h,\ v_h,\ u_h \in \mathbb{V}_h^k$, such that for all $\psi,\ \bar{\psi},\ \widetilde{\psi} \in \mathbb{V}_h^k$, it holds that

$$\int_{J_j}\int_{I_i} dw_h \psi dx dy = \int_{J_j}\int_{I_i} T_h \psi dx dy\, dt, \tag{3.27}$$

$$\int_{J_j}\int_{I_i} dv_h \bar{\psi} dx dy = \int_{J_j}\int_{I_i} S_h \bar{\psi} dx dy\, dt, \tag{3.28}$$

$$\int_{J_j}\int_{I_i} du_h \widetilde{\psi} dx dy = \int_{J_j}\int_{I_i} E_h \widetilde{\psi} dx dy\, dt, \tag{3.29}$$

which leads to the fact that $dw_h = T_h dt,\ dv_h = S_h dt,\ du_h = E_h dt$. Next, find $P_h,\ Q_h,\ R_h \in \mathbb{V}_h^k$ such that for any $\varphi,\ \widetilde{\varphi},\ \bar{\varphi} \in \mathbb{V}_h^k$, it holds that

$$\int_{J_j}\int_{I_i}(P_h - T_h)\varphi dxdy = \frac{1}{2}\int_{J_j}\left(\int_{I_i} u_h\varphi_x dx - (\widehat{u}_h\varphi^-)_{i+\frac{1}{2},y} + (\widehat{u}_h\varphi^+)_{i-\frac{1}{2},y}\right)dy, \tag{3.30}$$

$$\int_{J_j}\int_{I_i}(Q_h - S_h)\bar{\varphi} dxdy = -\frac{1}{2}\int_{I_i}\left(\int_{J_j} u_h\bar{\varphi}_y dy - (\widehat{u}_h\bar{\varphi}^-)_{x,j+\frac{1}{2}} + (\widehat{u}_h\bar{\varphi}^+)_{x,j-\frac{1}{2}}\right)dx, \tag{3.31}$$

$$\begin{aligned}\int_{J_j}\int_{I_i}(R_h - E_h)\widetilde{\varphi} dxdy &= \frac{1}{2}\int_{J_j}\left(\int_{I_i} w_h\widetilde{\varphi}_x dx - (\widehat{w}_h\widetilde{\varphi}^-)_{i+\frac{1}{2},y} + (\widehat{w}_h\widetilde{\varphi}^+)_{i-\frac{1}{2},y}\right)dy\\ &\quad - \frac{1}{2}\int_{I_i}\left(\int_{J_j} v_h\widetilde{\varphi}_y dy - (\widehat{v}_h\widetilde{\varphi}^-)_{x,j+\frac{1}{2}} + (\widehat{v}_h\widetilde{\varphi}^+)_{x,j-\frac{1}{2}}\right)dx,\end{aligned} \tag{3.32}$$

where the numerical fluxes are chosen as

$$(\widehat{u}_h)_{x_0,y} = (\{u_h\} - 2m_1[u_h])_{x_0,y},\ (\widehat{w}_h)_{x_0,y} = (\{w_h\} - 2n_1[w_h])_{x_0,y},\ \ m_n,\ n_2 \in \mathbb{R} \text{ with } m_1 - n_1 = \alpha_1,$$
$$(\widehat{u}_h)_{x,y_0} = (\{u_h\} + 2m_2[u_h])_{x,y_0},\ (\widehat{v}_h)_{x,y_0} = (\{v_h\} + 2n_2[u_h])_{x,y_0},\ \ m_n,\ n_2 \in \mathbb{R} \text{ with } m_2 - n_2 = \alpha_2.$$

By combining the derivative of (3.30)-(3.32) with the equations (3.2)-(3.4), we obtain

$$\begin{aligned}\int_{J_j}\int_{I_i} dP_h\phi dxdy &= -\frac{1}{2}\int_{J_j}\left(\int_{I_i} E_h\phi_x dx - (\widehat{E}_h\phi^-)_{i+\frac{1}{2},y} + (\widehat{E}_h\phi^+)_{i-\frac{1}{2},y}\right)dydt + \lambda_2\int_{J_j}\int_{I_i}\phi dW_t dxdy,\\ \int_{J_j}\int_{I_i} dQ_h\bar{\phi} dxdy &= \frac{1}{2}\int_{I_i}\left(\int_{J_j} E_h\bar{\phi}_y dy - (\widehat{E}_h\bar{\phi}^-)_{x,j+\frac{1}{2}} + (\widehat{E}_h\bar{\phi}^+)_{x,j-\frac{1}{2}}\right)dxdt + \lambda_2\int_{J_j}\int_{I_i}\bar{\phi} dW_t dxdy,\\ \int_{J_j}\int_{I_i} dR_h\widetilde{\phi} dxdy &= -\frac{1}{2}\int_{J_j}\left(\int_{I_i} T_h\widetilde{\phi}_x dx - (\widehat{T}_h\widetilde{\phi}^-)_{i+\frac{1}{2},y} + (\widehat{T}_h\widetilde{\phi}^+)_{i-\frac{1}{2},y}\right)dy\\ &\quad + \frac{1}{2}\int_{I_i}\left(\int_{J_j} S_h\widetilde{\phi}_y dy - (\widehat{S}_h\widetilde{\phi}^-)_{x,j+\frac{1}{2}} + (\widehat{S}_h\widetilde{\phi}^+)_{x,j-\frac{1}{2}}\right)dx - \lambda_1\int_{J_j}\int_{I_i}\widetilde{\phi} dW_t dxdy,\end{aligned} \tag{3.33}$$

where the numerical fluxes are

$$(\widehat{T}_h)_{x_0,y} = (\{T_h\} + 2m_1[T_h])_{x_0,y},\ \ (\widehat{E}_h)_{x_0,y} = (\{E_h\} + 2n_1[E_h])_{x_0,y},$$
$$(\widehat{E}_h)_{x,y_0} = (\{E_h\} - 2n_2[E_h])_{x,y_0},\ \ (\widehat{S}_h)_{x,y_0} = (\{S_h\} - 2m_2[S_h])_{x,y_0}.$$

Combining (3.27)-(3.33), we have derived the equivalent formulation of the DG scheme (3.2)-(3.4) for the new system (3.25): find $z_h \in (\mathbb{V}_h^k)^9$, such that for all $\boldsymbol{\varphi} \in (\mathbb{V}_h^k)^9$, we have

$$\begin{aligned}&\int_{J_j}\int_{I_i} M dz_h\cdot\boldsymbol{\varphi} dxdy - \int_{J_j}\Big(\int_{I_i} K_1 z_h\cdot\boldsymbol{\varphi}_x dx - \big(\widehat{K_1 z_h}\cdot\boldsymbol{\varphi}^-\big)_{i+\frac{1}{2},y} + \big(\widehat{K_1 z_h}\cdot\boldsymbol{\varphi}^+\big)_{i-\frac{1}{2},y}\Big)dydt\\ &-\int_{I_i}\Big(\int_{J_j} K_2 z_h\cdot\boldsymbol{\varphi}_y dy - \big(\widehat{K_2 z_h}\cdot\boldsymbol{\varphi}^-\big)_{x,j+\frac{1}{2}} + \big(\widehat{K_2 z_h}\cdot\boldsymbol{\varphi}^+\big)_{x,j-\frac{1}{2}}\Big)dxdt\\ &=\int_{J_j}\int_{I_i}\nabla S_1(z_h)\cdot\boldsymbol{\varphi} dxdydt + \int_{J_j}\int_{I_i}\nabla S_2(z_h)\cdot\boldsymbol{\varphi} dW_t dxdy,\end{aligned} \tag{3.34}$$

where $(\widehat{K_1 z_h})_{x_0,y} = (K_1\{z_h\} + A_1[z_h])_{x_0,y}$, and $(\widehat{K_2 z_h})_{x,y_0} = (K_2\{z_h\} + A_2[z_h])_{x,y_0}$,

$$A_1 = \begin{pmatrix} 0 & 0 & 0 & 0 & 0 & m_1 & 0 & 0 & 0 \\ 0 & 0 & 0 & 0 & 0 & 0 & 0 & 0 & 0 \\ 0 & 0 & 0 & n_1 & 0 & 0 & 0 & 0 & 0 \\ 0 & 0 & n_1 & 0 & 0 & 0 & 0 & 0 & 0 \\ 0 & 0 & 0 & 0 & 0 & 0 & 0 & 0 & 0 \\ m_1 & 0 & 0 & 0 & 0 & 0 & 0 & 0 & 0 \\ 0 & 0 & 0 & 0 & 0 & 0 & 0 & 0 & 0 \\ 0 & 0 & 0 & 0 & 0 & 0 & 0 & 0 & 0 \\ 0 & 0 & 0 & 0 & 0 & 0 & 0 & 0 & 0 \end{pmatrix}, \quad A_2 = \begin{pmatrix} 0 & 0 & 0 & 0 & 0 & 0 & 0 & 0 & 0 \\ 0 & 0 & 0 & 0 & 0 & m_2 & 0 & 0 & 0 \\ 0 & 0 & 0 & 0 & n_2 & 0 & 0 & 0 & 0 \\ 0 & 0 & 0 & 0 & 0 & 0 & 0 & 0 & 0 \\ 0 & 0 & n_2 & 0 & 0 & 0 & 0 & 0 & 0 \\ 0 & m_2 & 0 & 0 & 0 & 0 & 0 & 0 & 0 \\ 0 & 0 & 0 & 0 & 0 & 0 & 0 & 0 & 0 \\ 0 & 0 & 0 & 0 & 0 & 0 & 0 & 0 & 0 \\ 0 & 0 & 0 & 0 & 0 & 0 & 0 & 0 & 0 \end{pmatrix}.$$

Applying the exterior derivative to this scheme (3.34) leads to the variation equation

$$\begin{aligned} &\int_{J_j}\int_{I_i} M dZ_h \cdot \boldsymbol{\varphi} dxdy - \int_{J_j}\Big(\int_{I_i} K_1 Z_h \cdot \boldsymbol{\varphi}_x dx - \big(\widehat{K_1 Z_h}\cdot\boldsymbol{\varphi}^-\big)_{i+\frac{1}{2},y} + \big(\widehat{K_1 Z_h}\cdot\boldsymbol{\varphi}^+\big)_{i-\frac{1}{2},y}\Big)dydt \\ &-\int_{I_i}\Big(\int_{J_j} K_2 z_h \cdot \boldsymbol{\varphi}_y dy - \big(\widehat{K_2 Z_h}\cdot\boldsymbol{\varphi}^-\big)_{x,j+\frac{1}{2}} + \big(\widehat{K_2 Z_h}\cdot\boldsymbol{\varphi}^+\big)_{x,j-\frac{1}{2}}\Big)dxdt = \int_{J_j}\int_{I_i} \nabla^2 S_1 Z_h \cdot \boldsymbol{\varphi} dxdydt, \end{aligned} \tag{3.35}$$

Theorem 3.4 (***Conservation of multi-symplecticity***). *Let U_h, V_h be any solutions to the variational equation (3.35), we have the semi-discrete version of the multi-symplectic conservation laws*

$$\begin{aligned} &\int_{J_j}\int_{I_i} d(MU_h \cdot V_h)dx - \int_{J_j}\Big(\mathcal{F}_{K_1}(U_h,V_h)_{i+\frac{1}{2},y} - \mathcal{F}_{K_1}(U_h,V_h)_{i-\frac{1}{2},y}\Big)dydt \\ &\qquad -\int_{I_i}\Big(\mathcal{F}_{K_2}(U_h,V_h)_{x,j+\frac{1}{2}} - \mathcal{F}_{K_2}(U_h,V_h)_{x,j-\frac{1}{2}}\Big)dxdt = 0. \end{aligned} \tag{3.36}$$

The proof follows the same idea as that of Theorem 2.4, and is skipped here to save space.

4. Symplectic time discretization

In this section, we discuss the symplectic temporal discretization for the semi-discrete DG methods presented in the previous section.

In the one-dimensional case, we can set $\eta_h|_{I_j} = \sum_{l=0}^{k} \eta_j^l \varphi_j^l$, $u_h|_{I_j} = \sum_{l=0}^{k} u_j^l \varphi_j^l$, with the set $\{\varphi_j^l\}$ being the basis of V_h^k, and introduce the notations

$$p = (\eta_1^0, \cdots, \eta_1^k, \eta_2^0, \cdots, \eta_2^k, \cdots, \eta_J^k)^T, \quad q = (u_1^0, \cdots, u_1^k, u_2^0, \cdots, u_2^k, \cdots, u_J^k)^T.$$

In the two-dimensional case, we consider

$$E_h|_{I_i\times J_j} = \sum_{l=0}^{k^2+2k} E_{i,j}^l \varphi_{i,j}^l, \quad S_h|_{I_i\times J_j} = \sum_{l=0}^{k^2+2k} S_{i,j}^l \varphi_{i,j}^l, \quad T_h|_{I_i\times J_j} = \sum_{l=0}^{k^2+2k} T_{i,j}^l \varphi_{i,j}^l,$$

where $\{\varphi_{i,j}^l\}$ is the basis of $\mathbb{V}_h^k$. Define

$$\begin{aligned} &E_{i,j} = (E_{i,j}^0, E_{i,j}^1, \cdots, E_{i,j}^{k^2+2k})^T, \\ &\boldsymbol{E}_h = \big(E_{1,1}, E_{2,1}, \cdots, E_{I,1}, E_{1,2}, \cdots, E_{I,J}\big)^T, \end{aligned}$$

and similarly for $\boldsymbol{S}_h$, $\boldsymbol{T}_h$, and then introduce the notations

$$p = \boldsymbol{E}_h, \qquad q = (\boldsymbol{S}_h,\ \boldsymbol{T}_h)^T.$$

With these notations, either the one-dimensional scheme (2.2)-(2.3) or the two-dimensional method (3.2)-(3.4) can be simplified into the following stochastic differential equations

$$dp = Aq + L\sum_{m=1}^{\infty} d\mathcal{B}_m(t), \qquad dq = Bp + N\sum_{m=1}^{\infty} d\mathcal{B}_m(t),$$

where A, B, L, N are some constant matrices which may take different values in 1D or 2D setting. In this section, it is sufficient to consider the simplified version of it

$$dp = Aq + Ld\mathcal{B}_t, \qquad dq = Bp + Nd\mathcal{B}_t, \tag{4.1}$$

where $\mathcal{B}_t$ is a Brownian motion.

Remark 4.1. As studied in [29, Theorem 4.1], a suitable symplectic Runge-Kutta time integration, combined with the DG spatial discretization, leads to a multi-symplectic scheme for HPDEs which is equivalent to a time-space PRK scheme for this model. Therefore, two symplectic temporal integration methods will be discussed below.

4.1. Symplectic Euler method

We let $0 = t_0 \le t_1 \le \cdots \le t_N = T$ be a partition of the time interval $[0, T]$. By setting $\tau = t_{k+1} - t_k$, and $\Delta\mathcal{B}_k = \mathcal{B}_{t_{k+1}} - \mathcal{B}_{t_k}$, the symplectic Euler methods for the system (4.1) are given by

$$p^{k+1} = p^k + \tau Aq^k + L\Delta\mathcal{B}_k, \qquad q^{k+1} = q^k + \tau Bp^{k+1} + N\Delta\mathcal{B}_k. \tag{4.2}$$

Following the studies in [22], we have the following result:

Theorem 4.1. *Symplectic Euler method (4.2) has the first mean-square order of convergence.*

4.2. Partitioned Runge-Kutta method

Consider the two-stage symplectic PRK methods [22] for the system (4.1) of the form

$$\begin{aligned}
\mathcal{Q}_1 &= q^k + N\Big(J_k + \frac{1}{\sqrt{2}}\Delta\mathcal{B}_k\Big)\\
\mathcal{P}_1 &= p^k + \frac{1}{4}\tau A\mathcal{Q}_1 + L\Big(J_k + \frac{1}{2\sqrt{3}}\Delta\mathcal{B}_k\Big),\\
\mathcal{Q}_2 &= q^k + \frac{2}{3}\tau B\mathcal{P}_1 + \Delta\mathcal{B}_k N\Big(J_k - \frac{1}{3\sqrt{2}}\Delta\mathcal{B}_k\Big),\\
\mathcal{P}_2 &= p^k + \tau\Big(\frac{1}{4}A\mathcal{Q}_1 + \frac{3}{4}A\mathcal{Q}_2\Big) + L\Big(J_k - \frac{1}{\sqrt{3}}\Delta\mathcal{B}_k\Big),\\
p^{k+1} &= p^k + L\Delta\mathcal{B}_k + \tau\Big(\frac{1}{4}A\mathcal{Q}_1 + \frac{3}{4}A\mathcal{Q}_2\Big)\\
q^{k+1} &= q^k + N\Delta\mathcal{B}_k + \tau\Big(\frac{2}{3}B\mathcal{P}_1 + \frac{1}{3}B\mathcal{P}_2\Big),
\end{aligned} \tag{4.3}$$

where

$$\tau = t_{k+1} - t_k, \qquad \Delta\mathcal{B}_k = \mathcal{B}_{t_{k+1}} - \mathcal{B}_{t_k}, \qquad J_k = \frac{1}{\tau}\int_{t_k}^{t_{k+1}} \mathcal{B}_s - \mathcal{B}_{t_k} ds.$$

The random variables $\Delta\mathcal{B}_k$ and J_k are modeled numerically at each step following the approach discussed in [15], where a new process

$$v(s) = \frac{W_{t_k+\tau s} - W_{t_k}}{\sqrt{\tau}}, \qquad 0 \le s \le 1$$

is introduced and we have $\Delta\mathcal{B}_k = \sqrt{\tau}v(1)$ and $J_k = \sqrt{\tau^3}\int_0^1 v(s)ds$. Therefore, they can be computed numerically by solving for $v(s)$ numerically, and we refer to [15, Section 4.2.2] for the details of the implementation.

In order to analyze the convergence rate of the PRK methods (4.3), we recall the following theorem in [20, Theorem 1.1].

Theorem 4.2. *Consider a general system of stochastic differential equation*

$$dX = a(t, X)dt + \sum_{r=1}^{m} b_r(t, X)d\mathcal{B}_r(t), \tag{4.4}$$

where X, a and b_r are column vectors defined on $t \in [t_0, T]$, and $\mathcal{B}_r$ are independent standard Brownian motions, and let $\overline{X}_{t,x}(t+\tau)$ be a one-step approximation satisfying that for any $t_0 \le t \le T - \tau$,

$$\left|\mathbb{E}\Big(X_{t,x}(t+\tau)-\overline{X}_{t,x}(t+\tau)\Big)\right| \le K(1+|x|^2)^{1/2}\tau^{p_1}, \tag{4.5}$$

$$\left(\mathbb{E}\left|X_{t,x}(t+\tau)-\overline{X}_{t,x}(t+\tau)\right|^2\right)^{1/2} \le K(1+|x|^2)^{1/2}\tau^{p_2}. \tag{4.6}$$

Let $p_2 \ge \frac{1}{2}$, $p_1 \ge p_2+\frac{1}{2}$, then for any N and $k=0,1,\cdots,N$, the following result holds:

$$\left(\mathbb{E}\left|X_{t_0,X_0}(t_k)-\overline{X}_{t_0,X_0}(t_k)\right|^2\right)^{1/2} \le K(1+\mathbb{E}|X_0|^2)^{1/2}\tau^{p_2-\frac{1}{2}}. \tag{4.7}$$

The following Lemma, which is also studied in [21, Lemma 2.1], is a direct result of Theorem 4.2 and will be useful in our analysis.

Lemma 4.1. *Let the one-step approximation $\overline{X}_{t,x}(t+\tau)$ satisfies the conditions of Theorem 4.2, and suppose that another one step approximation $\widetilde{X}_{t,x}(t+\tau)$ satisfies*

$$\left|\mathbb{E}\Big(\widetilde{X}_{t,x}(t+\tau)-\overline{X}_{t,x}(t+\tau)\Big)\right| = O(\tau^{p_1}), \tag{4.8}$$

$$\left(\mathbb{E}\left|\widetilde{X}_{t,x}(t+\tau)-\overline{X}_{t,x}(t+\tau)\right|^2\right)^{1/2} = O(\tau^{p_2}), \tag{4.9}$$

with the same p_1 and p_2 as in Theorem 4.2, then the mean-square order of accuracy for $\widetilde{X}_{t,x}(t+\tau)$ is also $p_2-1/2$, same as $\overline{X}_{t,x}(t+\tau)$.

We have the following main result on the convergence rate of the PRK method (4.3).

Theorem 4.3. *The explicit PRK method (4.3) for the system (4.1) has the mean-square order of 2.*

Proof. According to [14, Section 10.5], the following one-step approximation for the system (4.1) has the mean-square order 2:

$$\overline{p}^{k+1} = p^k + \tau Aq^k + \frac{1}{2}\tau^2 ABp^k + \tau AN J_k + L\Delta\mathcal{B}_k, \tag{4.10}$$

$$\overline{q}^{k+1} = q^k + \tau Bp^k + \frac{1}{2}\tau^2 BAq^k + \tau BL J_k + N\Delta\mathcal{B}_k, \tag{4.11}$$

which will be used as a reference method.

The PRK method (4.3) can be rewritten as

$$p^{k+1} = p^k + \tau Aq^k + \frac{1}{2}\tau^2 ABp^k + \tau AN J_k + L\Delta\mathcal{B}_k + \frac{1}{2}\tau^2 ABL\Big(J_k + \frac{1}{2\sqrt{3}}\Delta\mathcal{B}_k\Big) + O(\tau^3),$$

$$q^{k+1} = q^k + \tau Bp^k + \frac{1}{2}\tau^2 BAq^k + \tau BL J_k + N\Delta\mathcal{B}_k + \frac{1}{2}\tau^2 BAN\Big(J_k + \frac{1}{3\sqrt{2}}\Delta\mathcal{B}_k\Big) + O(\tau^3).$$

Notice that

$$\mathbb{E}J_k = \mathbb{E}\Delta\mathcal{B}_k = 0, \qquad \mathbb{E}(J_k)^2 = \frac{\tau}{3}, \qquad \mathbb{E}(\Delta\mathcal{B}_k)^2 = \tau,$$

which, by Young's inequality, leads to

$$\mathbb{E}\Big(J_k + \frac{1}{2\sqrt{3}}\Delta\mathcal{B}_k\Big)^2 \le C\mathbb{E}(J_k)^2 + C\mathbb{E}(\Delta\mathcal{B}_k)^2 = O(\tau).$$

Therefore, we have

$$\left|\mathbb{E}\Big(p^{k+1}-\overline{p}^{k+1}\Big)\right| = O(\tau^3),$$

$$\mathbb{E}\Big(p^{k+1}-\overline{p}^{k+1}\Big)^2 = \mathbb{E}\Big(\frac{1}{2}\tau^2 ABL\Big(J_k + \frac{1}{2\sqrt{3}}\Delta\mathcal{B}_k\Big) + O(\tau^3)\Big)^2 = O(\tau^5),$$

Table 5.1
Numerical error and convergence rates of 1D case when $k = 1$.

Nx	Nt	$\|e_u\|$	order	$\|e_\eta\|$	order
20	600	0.01295	0	0.01725	0
40	1200	3.201E-3	2.0162	4.281E-3	2.0106
80	2400	7.851E-4	2.0276	1.083E-3	1.9829
160	4800	1.958E-4	2.0036	2.714E-4	1.9966

Table 5.2
Numerical error and convergence rates of 1D case when $k = 2$.

Nx	Nt	$\|e_u\|$	order	$\|e_\eta\|$	order
20	600	3.176E-4	0	4.407E-4	0
40	1200	3.958E-5	3.0045	5.486E-5	3.0061
80	2400	4.920E-6	3.0081	6.874E-6	2.9964
160	4800	6.144E-7	3.0013	8.645E-7	2.9912

which leads to

$$\left(\mathbb{E}\left(p^{k+1} - \overline{p}^{k+1}\right)^2\right)^{1/2} = O(\tau^{5/2}).$$

Following a similar approach, we also have

$$\left|\mathbb{E}\left(q^{k+1} - \overline{q}^{k+1}\right)\right| = O(\tau^3), \qquad \left(\mathbb{E}\left(q^{k+1} - \overline{q}^{k+1}\right)^2\right)^{1/2} = O(\tau^{5/2}).$$

Therefore, by applying the result of Lemma 4.1, the PRK method (4.3) has mean-square order of 2. □

Remark 4.2. The PRK scheme (4.3) was shown in [22] to have the mean-square order of 3/2 for general system. For this linear system (4.1), it can be shown to have second order mean-square convergence rate.

5. Numerical experiments

The numerical results of the DG scheme is presented in this section to demonstrate the performance of the proposed methods. We consider the DG method with various polynomial degree k as the spatial discretization, and utilize the PRK method (4.3) for temporal discretization. The accuracy tests are provided for both 1D case and 2D case to demonstrate the convergence rate of the methods, and the linear growth of discrete energy is also studied for both cases.

5.1. Accuracy test

5.1.1. Example 1

For the one-dimensional system (2.1) with periodic boundary conditions, we set $\lambda_1 = \lambda_2 = 1$, and choose $W_t = \mathcal{B}_t$, which is the standard Brownian motion, so that one exact solution to (2.1) takes the form

$$\begin{cases} \eta = \sin(x - t) + \cos(x + t) - \mathcal{B}_t \\ u = \sin(x - t) - \cos(x + t) + \mathcal{B}_t. \end{cases} \tag{5.1}$$

The computational domain is $[0, 2\pi]$ and the final time is set to $T = 3$. Initial conditions for $\eta(x, 0)$ and $u(x, 0)$ are obtained by letting $t = 0$ in (5.1). We use Nx and Nt to denote number of spatial cells and temporal steps respectively. Table 5.1 and Table 5.2 demonstrates the order of convergence rate for the case $k = 1$ and $k = 2$ respectively, where Δt is chosen to be small enough to ensure that the spatial error dominates. Under both cases, we can observe the optimal convergence orders, i.e., $(k+1)$-th order of accuracy, which is consistent with the result in Theorem 2.3 for the semi-discrete method. Note that the second order temporal discretization is used for both cases, therefore, one would expect a second order convergence even coupled with third order DG spatial discretization. This second order convergence is observed in Table 5.3, when larger Δt is used.

5.1.2. Example 2

Next, we consider the two-dimensional stochastic Maxwell equations (3.1) with periodic boundary conditions. Set $\lambda_1 = \lambda_2 = 1$, and choose $W_t = \mathcal{B}_t$, then the exact solution to (3.1) takes the form

Table 5.3
Numerical error and convergence rates of 1D case when $k=2$ with larger Δt.

Nx	Nt	$\|e_u\|$	order	$\|e_\eta\|$	order
20	60	5.6019E-4	0	5.3547E-4	0
40	120	1.2175E-4	2.2020	9.5595E-5	2.4858
80	240	2.9228E-5	2.0585	2.0804E-5	2.2000
160	480	7.2337E-6	2.0145	4.9803E-6	2.0626

Table 5.4
Numerical error and convergence rates of 2D case when $k=1$.

Nx	Ny	Nt	$\|e_E\|$	order	$\|e_S\|$	order	$\|e_T\|$	order
20	20	200	0.02715	0	0.01749	0	0.01749	0
40	40	400	6.617E-3	2.0366	4.466E-3	1.9696	4.466E-3	1.9696
80	80	800	1.634E-3	2.0176	1.129E-3	1.9839	1.129E-3	1.9839
160	160	1600	4.061E-4	2.0086	2.839E-4	1.9918	2.839E-4	1.9918

Table 5.5
Numerical error and convergence rates of 2D case when $k=2$.

Nx	Ny	Nt	$\|e_E\|$	order	$\|e_S\|$	order	$\|e_T\|$	order
20	20	200	8.529E-4	0	5.899E-4	0	5.899E-4	0
40	40	400	9.980E-5	3.0952	7.061E-5	3.0628	7.061E-5	3.0628
80	80	800	1.253E-5	2.9939	9.119E-6	2.9529	9.119E-6	2.9529
160	160	1600	1.521E-6	3.0422	1.137E-6	3.0038	1.137E-6	3.0038

$$\begin{cases} E = \sin(x+t) - \cos(y+t) - \mathcal{B}_t, \\ S = \cos(y+t) + \mathcal{B}_t, \\ T = \sin(x+t) + \mathcal{B}_t. \end{cases} \tag{5.2}$$

The spatial domain is set to be $[0, 2\pi]^2$, and the final stopping time is taken to be $T=1$. The initial conditions of E, S, T can be obtained by setting $t=0$ in the exact solutions (5.2). We use Nx and Nt to denote number of spatial cells and temporal steps respectively. The numerical errors and the corresponding convergence rates are shown in Table 5.4 for $k=1$ and in Table 5.5 for $k=2$. Under both cases, we can observe the optimal convergence orders, i.e., $(k+1)$-th order of accuracy, which matches the analysis in Theorem 3.3 for the semi-discrete method.

5.1.3. Example 3

Finally in this section we consider the one-dimensional system (2.1) with space-time mixed noise and periodic boundary condition. Let $\lambda_1 = \lambda_2 = 1$ and consider the initial condition

$$\begin{cases} \eta(x,0) = \sin(x) + \cos(x), \\ u(x,0) = \sin(x) - \cos(x). \end{cases}$$

The computational domain is $I = [0, 2\pi]$ and we set final time $T = 0.1$. W_t is the space-time mixed Wiener process defined as

$$W_t = \sum_{m=1}^{\infty} \sqrt{\frac{1}{m^3}} \frac{\sin(mx)}{\sqrt{\pi}} \mathcal{B}_m, \tag{5.3}$$

which is truncated by taking the sum over m up to 100 numerically.

Since the exact solution is not available, we compute a set of reference solutions u^{ref}, η^{ref} using the refined 10240 spatial computational cells and 102400 time steps. We first generate the random variables $\Delta\mathcal{B}_k^{ref}$ and $J_k^{ref} = \frac{1}{\tau^{ref}} \int_{t_k}^{t_{k+1}} \mathcal{B}_s - \mathcal{B}_{t_k} ds$ on each refined time step. The same discretized Brownian path, but with (a large) time step size τ, is used to compute the numerical solution. For example, assuming the time interval $[t_k, t_k + \tau]$ with larger τ can be written as $[t_k, t_k + r\tau^{ref}]$, we can evaluate $\Delta\mathcal{B}_k$, J_k from the reference ones, by observing that

$$\Delta\mathcal{B}_k = \sum_{i=0}^{r-1} \Delta\mathcal{B}_{k+i}^{ref}, \qquad J_k = \frac{1}{\tau} \sum_{i=0}^{r-1} \int_{t_{k+i}}^{t_{k+i+1}} \mathcal{B}_s ds - \mathcal{B}_{t_k} = \frac{1}{\tau} \sum_{i=0}^{r-1} \left(\tau^{ref} (J_{k+i}^{ref} + \mathcal{B}_{t_{k+i}}) \right) - \mathcal{B}_{t_k}.$$

Table 5.6 shows the numerical errors and the corresponding convergence rates for the case $k=2$, and we can observe the optimal rate of convergence ($k+1$ th order of accuracy) for this case with space-time mixed noise, which is consistent with the analytical result in Theorem 2.3.

Table 5.6
Numerical error and convergence rates of 1D case when $k = 2$ for space-time mixed noise.

Nx	Nt	$\|e_u\|$	order	$\|e_\eta\|$	order
320	3200	7.9988E-4	0	8.1094E-4	0
640	6400	9.5457E-5	3.0688	8.9730E-5	3.1759
1280	12800	1.2232E-5	2.9642	1.1932E-5	2.9107
2560	25600	1.4548E-6	3.0719	1.4801E-6	3.0112

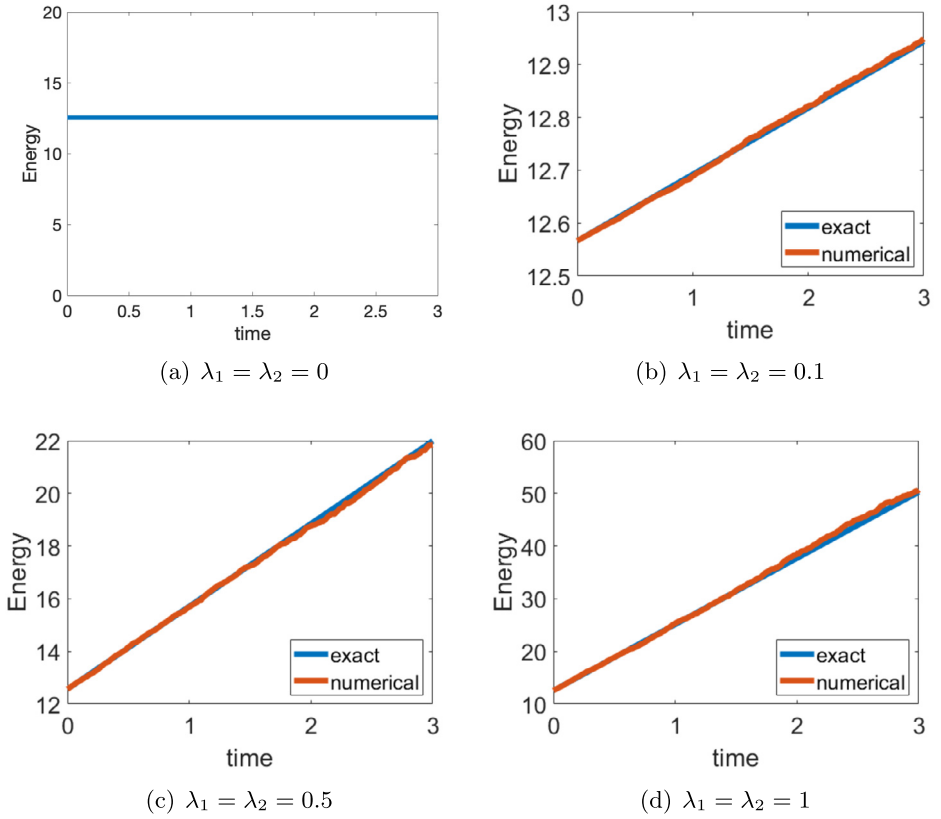

(a) $\lambda_1 = \lambda_2 = 0$ (b) $\lambda_1 = \lambda_2 = 0.1$

(c) $\lambda_1 = \lambda_2 = 0.5$ (d) $\lambda_1 = \lambda_2 = 1$

Fig. 5.1. Averaged energy with different sizes of noise for 1D case. (For interpretation of the colors in the figure(s), the reader is referred to the web version of this article.)

5.2. Averaged energy growth

The discrete energy law satisfied by the numerical solutions u_h and η_h was studied in Theorem 2.2 for the one-dimensional system. Under the same setup of initial condition, noise and boundary condition as in Example 1 and Example 2 in Section 5.1, we simulate the system up to the final stopping time $T = 3$, with the time step size $\Delta t = 0.0075$ and 80 space meshes. In this test, we run the simulations with 2000 samples, and take the average to approximate the expectation and compute the averaged energy. Fig. 5.1 shows the time history of the averaged energy of our numerical solutions together with exact solutions with different noise size $\lambda_{1,2}$, from which we can observe that the averaged energy of numerical solutions is almost linear with respect to time. Note that when $\lambda_1 = \lambda_2 = 0$, the global energy is preserved exactly on the discrete level. When the noise sizes $\lambda_{1,2}$ increase, the linear growth rate of the discrete energy also increases. The slopes of the discrete energy in Fig. 5.1 (b-d) can be computed via least square fitting, and are approximately 0.1228, 3.085, 12.987 respectively. They are proportional to $\lambda_1^2 + \lambda_2^2$, which is consistent with the result in Theorem 2.2. From Fig. 5.1 we can also observe that the discrete energy growth is very close to the exact energy growth.

Similarly, Theorem 3.2 studied the discrete energy law satisfied by the numerical solutions E_h, S_h and T_h for the two-dimensional system. For this example we simulate the system up to the final stopping time $T = 1$, with the time step size $\Delta t = 0.0025$ and 80×80 space meshes. In this test, we run the simulations with 1000 samples, and take the average to approximate the expectation and compute the averaged energy. Fig. 5.2 shows the time history of the averaged energy of our numerical solutions and exact solutions with different noise size $\lambda_{1,2}$, from which we can observe that the averaged energy is almost linear with respect to time, and the lines are very close to those of exact solutions. Note that when $\lambda_1 = \lambda_2 = 0$, the global energy is preserved exactly on the discrete level. When the noise sizes $\lambda_{1,2}$ increase, the linear growth rate of

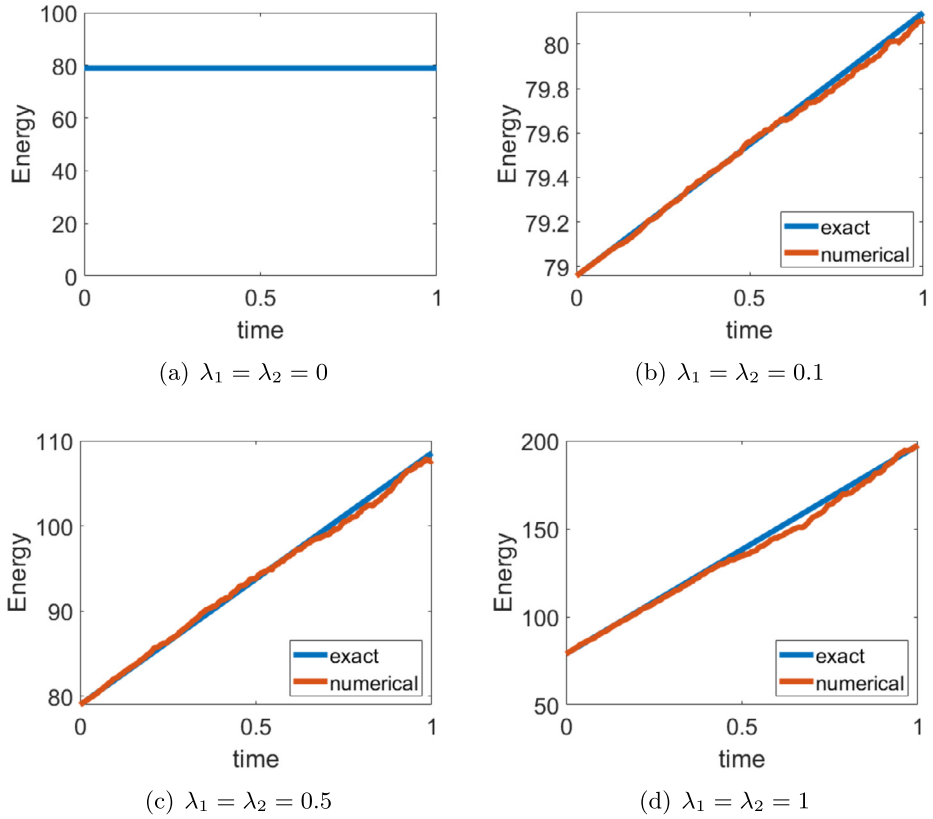

(a) $\lambda_1 = \lambda_2 = 0$ (b) $\lambda_1 = \lambda_2 = 0.1$

(c) $\lambda_1 = \lambda_2 = 0.5$ (d) $\lambda_1 = \lambda_2 = 1$

Fig. 5.2. Averaged energy with different sizes of noise for 2D case.

the discrete energy also increases. The slopes of the lines in Fig. 5.2 (b-d) can be computed via least square fitting, and are approximately 1.1413, 28.500, 115.08, respectively. They are proportional to $\lambda_1^2 + \lambda_2^2$, which is consistent with the result in Theorem 3.2.

5.3. Test with noises of various sizes

In this example, we consider the two-dimensional system (3.1), and use the initial conditions studied in [2]:

$$\begin{cases} E(x, y, 0) = \sin(3\pi x)\sin(4\pi y), \\ S(x, y, 0) = -\frac{4}{5}\cos(3\pi x)\cos(4\pi y), \\ T(x, y, 0) = -\frac{3}{5}\sin(3\pi x)\cos(4\pi y), \end{cases}$$

with $I \times J = [0, \frac{2}{3}] \times [0, \frac{1}{2}]$. The final stopping time is set as $T = 1$. Following the definition (1.5), we construct the Wiener process as

$$W_t = \sum_{m,n=1}^{\infty} 2\sqrt{\frac{3}{m^3 + n^3}} \sin\left(\frac{3}{2}m\pi x\right) \sin\left(2n\pi y\right) \mathcal{B}_{m,n}(t), \tag{5.4}$$

and truncate the sum (5.4) by taking the sum over m, n from 1 to 50.

In this example, the mesh sizes $\Delta x = \Delta y = 0.0083$ and time step size $\Delta t = 0.00083$ are considered. In order to show the effect of noise with various sizes on the numerical solution, we run the simulations with four sets of parameters: $\lambda_{1,2} = 0, 0.01, 0.05, 0.07$. The contour plots of the numerical solution S_h with these choices of noises are shown in Fig. 5.3. The 3D plots of T_h are also provided in Fig. 5.4. It can be observed from these figures that the perturbation of the numerical solutions becomes more and more obvious as the size of the noise grows.

5.4. Long-time behavior of solutions

In this example, we consider the one-dimensional model (2.1) with periodic boundary conditions and $W_t = \mathcal{B}_t$, and one possible traveling wave solution takes the form

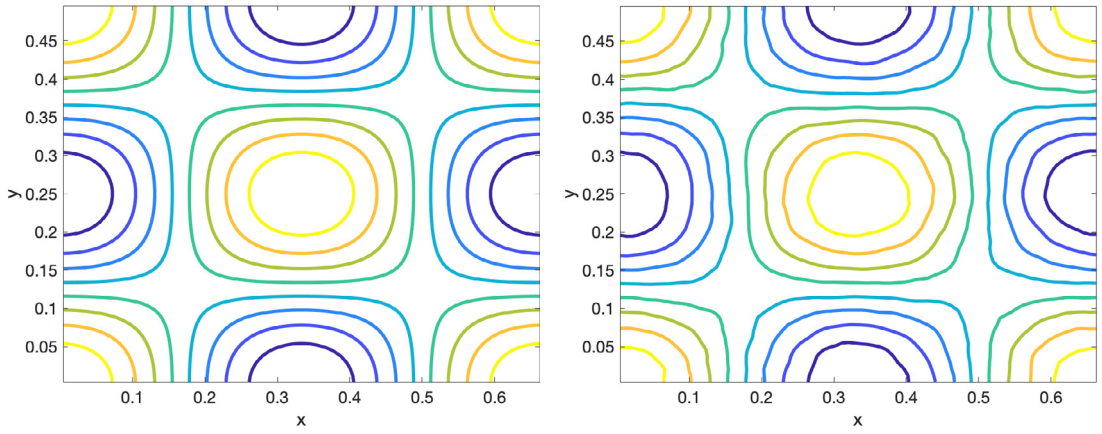

(a) $\lambda_1 = \lambda_2 = 0$ (b) $\lambda_1 = \lambda_2 = 0.01$

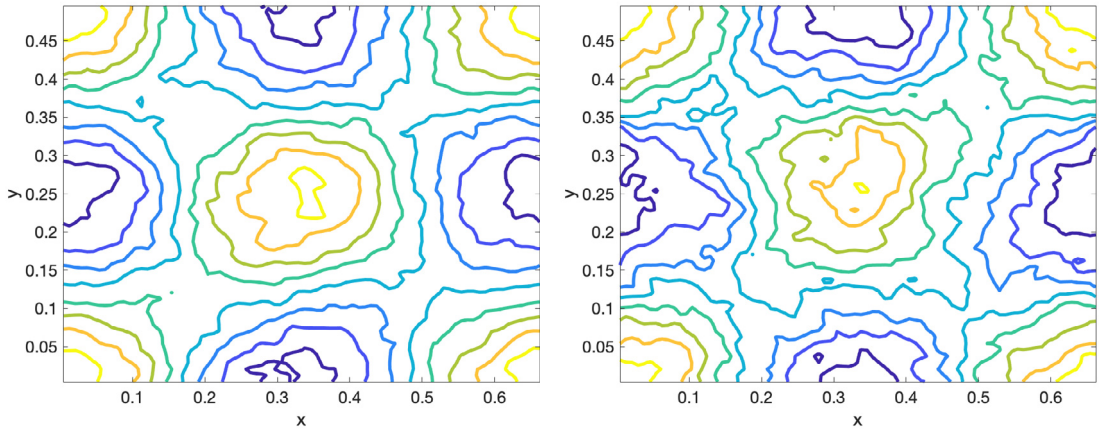

(c) $\lambda_1 = \lambda_2 = 0.05$ (d) $\lambda_1 = \lambda_2 = 0.07$

Fig. 5.3. Contour plots of $S_h(x, y)$ with different sizes of noise for the test in Section 5.3. 8 uniformly spaced contour lines within the range $[-0.8, 0.8]$ are used.

$$\begin{cases} \eta(x,t) = \operatorname{sech}^2(5(x-t)-15) - \lambda_1 \mathcal{B}_t, \\ u(x,t) = \operatorname{sech}^2(5(x-t)-15) + \lambda_2 \mathcal{B}_t. \end{cases} \tag{5.5}$$

The computation domain is set to be $[0, 6]$, with the mesh size $\Delta x = 0.0375$, and $\Delta t = 0.003125$. The initial condition is chosen to be the exact solution (5.5) with $t = 0$.

Fig. 5.5 shows the time history of the waveform numerical solutions u_h running up to final time $T = 28$ (almost 5 periods). We can observe that when there is no noise ($\lambda_1 = \lambda_2 = 0$), the shape and height of the wave does not change during the simulation, and when small noise exists ($\lambda_1 = \lambda_2 = 0.1$), the height of the wave is impacted by the noise.

Fig. 5.6 demonstrates the comparison of the numerical solution and the exact solution at different times. We choose $\lambda_1 = \lambda_2 = 0.1$, and run the simulation until $T = 103$. From Fig. 5.6 we can that the numerical solution almost coincides with the exact solution at different times, which means that our multi-symplectic DG scheme can preserve the shape and height of the wave accurately for a long time.

6. Conclusion remark

In this paper we have developed and analyzed the DG scheme for the one- and two-dimensional stochastic Maxwell equations with additive noise. The proposed methods are shown to satisfy the discrete form of the stochastic energy linear growth property. The optimal error estimate of the semi-discrete methods is also proven analytically. By introducing auxiliary variables, we also rewrite the stochastic Maxwell equations into the multi-symplectic structure and demonstrate that the proposed DG methods preserve the multi-symplectic structure. The semi-discrete methods are then combined with the symplectic Euler or PRK temporal discretization methods. Numerical experiments are provided to test the performance of the resulting methods, and optimal error estimates and linear growth of the discrete energy can be observed for all cases.

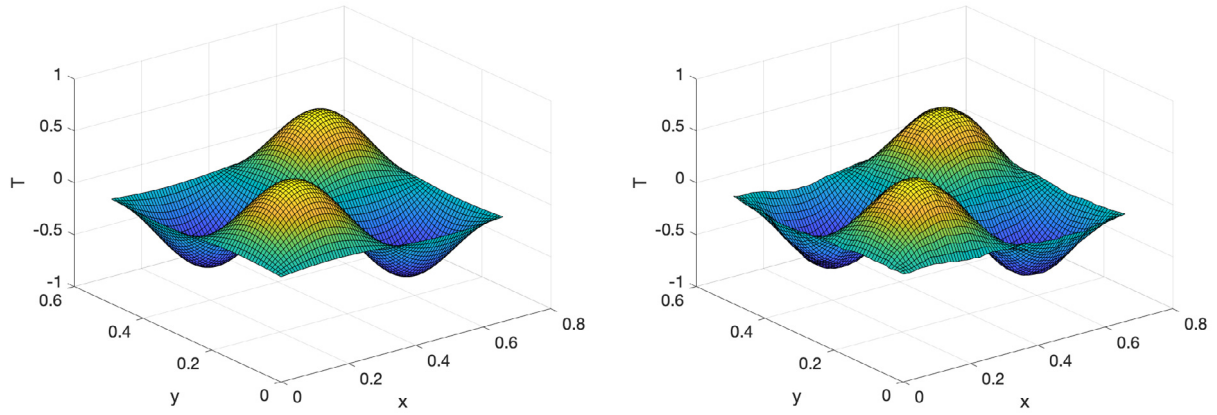

(a) $\lambda_1 = \lambda_2 = 0$ (b) $\lambda_1 = \lambda_2 = 0.01$

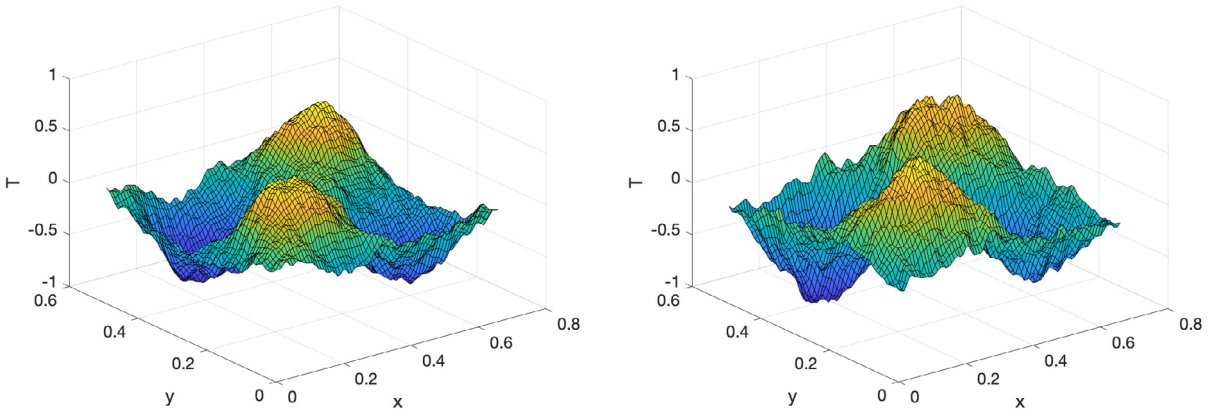

(c) $\lambda_1 = \lambda_2 = 0.05$ (d) $\lambda_1 = \lambda_2 = 0.07$

Fig. 5.4. 3D plots of $T_h(x, y)$ with different sizes of noise for the test in Section 5.3.

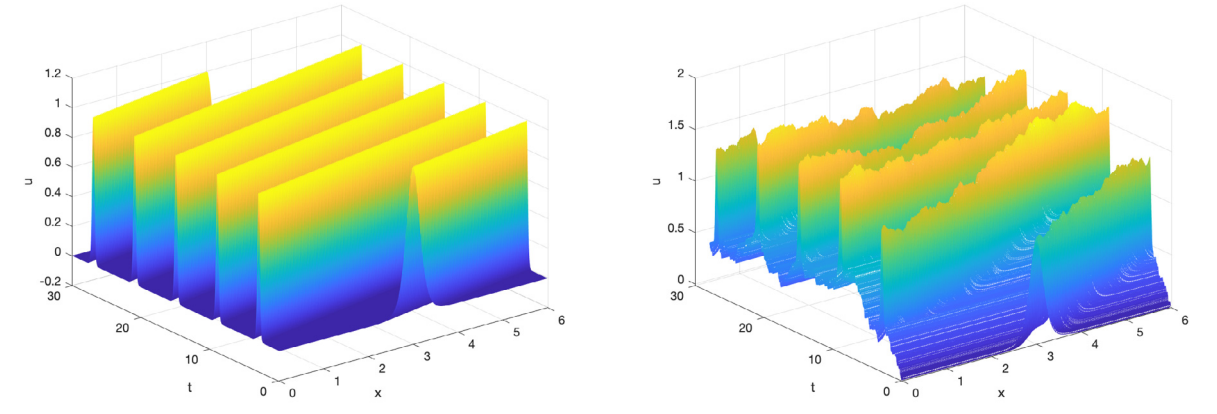

(a) $\lambda_1 = \lambda_2 = 0$ (b) $\lambda_1 = \lambda_2 = 0.1$

Fig. 5.5. 3D plots of the time history of the waveform of numerical solutions with or without noise.

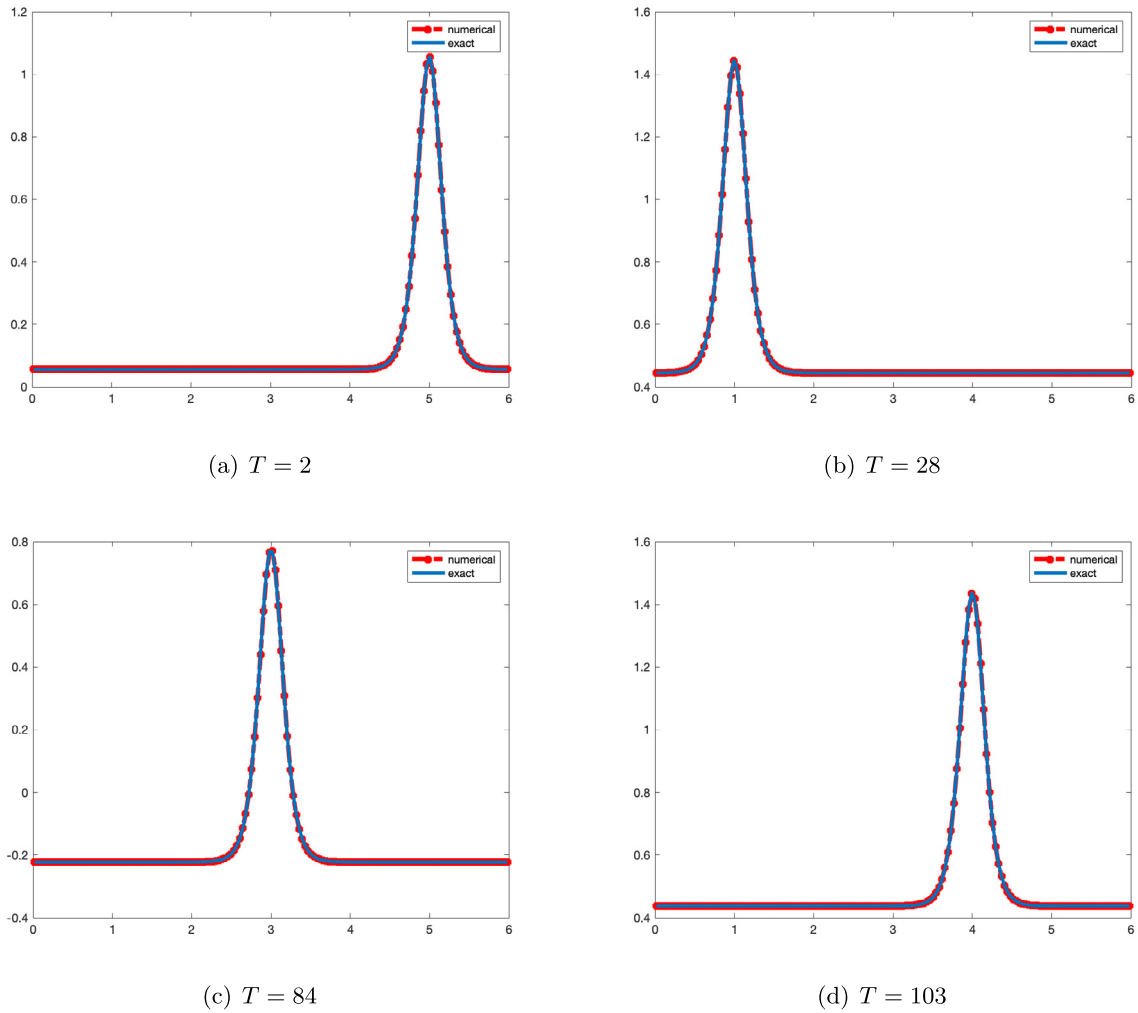

(a) $T = 2$ (b) $T = 28$

(c) $T = 84$ (d) $T = 103$

Fig. 5.6. Comparison between numerical solutions and exact solutions at different times.

CRediT authorship contribution statement

Jiawei Sun: Conceptualization, Methodology, Software, Validation, Writing, Visualization
Chi-Wang Shu: Conceptualization, Methodology, Supervision
Yulong Xing: Conceptualization, Methodology, Writing, Supervision

Declaration of competing interest

The authors declare that they have no known competing financial interests or personal relationships that could have appeared to influence the work reported in this paper.

References

[1] C. Chen, A symplectic discontinuous Galerkin full discretization for stochastic Maxwell equations, SIAM J. Numer. Anal. 59 (2021) 2197–2217.
[2] C. Chen, J. Hong, L. Zhang, Preservation of physical properties of stochastic Maxwell equations with additive noise via stochastic multi-symplectic methods, J. Comput. Phys. 306 (2016) 500–519.
[3] C. Chen, J. Hong, L. Ji, Runge-Kutta semidiscretizations for stochastic Maxwell equations with additive noise, SIAM J. Numer. Anal. 57 (2019) 702–727.
[4] C. Chen, J. Hong, J. Ji, Mean-square convergence of a semidiscrete scheme for stochastic Maxwell equations, SIAM J. Numer. Anal. 57 (2019) 728–750.
[5] Y. Cheng, C.-S. Chou, F. Li, Y. Xing, L2 stable discontinuous Galerkin methods for one-dimensional two-way wave equations, Math. Comput. 86 (2017) 121–155.
[6] B. Cockburn, S. Hou, C.-W. Shu, The Runge-Kutta local projection discontinuous Galerkin finite element method for conservation laws IV: the multidimensional case, Math. Comput. 54 (1990) 545–581.

[7] B. Cockburn, G. Karniadakis, C.-W. Shu, The development of discontinuous galerkin methods, in: B. Cockburn, G. Karniadakis, C.-W. Shu (Eds.), Discontinuous Galerkin Methods: Theory, Computation and Applications, in: Lecture Notes in Computational Science and Engineering, Part I: Overview, vol. 11, Springer, 2000, pp. 3–50.
[8] B. Cockburn, S.-Y. Lin, C.-W. Shu, TVB Runge-Kutta local projection discontinuous Galerkin finite element method for conservation laws III: one dimensional systems, J. Comput. Phys. 84 (1989) 90–113.
[9] B. Cockburn, C.-W. Shu, TVB Runge-Kutta local projection discontinuous Galerkin finite element method for conservation laws II: general framework, Math. Comput. 52 (1989) 411–435.
[10] D. Cohen, J. Cui, J. Hong, L. Sun, Exponential integrators for stochastic Maxwell's equations driven by Itô noise, J. Comput. Phys. 410 (2020) 109382.
[11] J. Hong, L. Ji, L. Zhang, A stochastic multi-symplectic scheme for stochastic Maxwell equations with additive noise, J. Comput. Phys. 268 (2014) 255–268.
[12] J. Hong, L. Ji, L. Zhang, J. Cai, An energy-conserving method for stochastic Maxwell equations with multiplicative noise, J. Comput. Phys. 351 (2017) 216–229.
[13] S. Jiang, L. Wang, J. Hong, Stochastic multi-symplectic integrator for stochastic nonlinear Schrödinger equation, Commun. Comput. Phys. 14 (2013) 393–411.
[14] P. Kloeden, E. Platen, Numerical Solution of Stochastic Differential Equations, 3rd ed., Applications in Mathematics, Stochastic Modelling and Applied Probability, vol. 23, Springer-Verlag, Berlin, 1999.
[15] Y. Li, C.-W. Shu, S. Tang, A discontinuous Galerkin method for stochastic conservation laws, SIAM J. Sci. Comput. 42 (2020) A54–A86.
[16] Y. Li, C.-W. Shu, S. Tang, An ultra-weak DG method with IMEX time-marching for generalized stochastic KdV equations, J. Sci. Comput. 82 (2020) 61.
[17] Y. Li, S. Wu, Y. Xing, Finite element approximations of a class of nonlinear stochastic wave equation with multiplicative noise, J. Sci. Comput. 91 (2022) 53.
[18] G. Liu, Stochastic wave propagation in Maxwell's equations, J. Stat. Phys. 158 (2015) 1126–1146.
[19] K.B. Liaskos, I.G. Stratis, A.N. Yannacopoulos, Stochastic integrodifferential equations in Hilbert spaces with applications in electromagnetics, J. Integral Equ. Appl. 22 (2010) 559–590.
[20] G.N. Milstein, Numerical Integration of Stochastic Differential Equations, Mathematics and Its Applications, vol. 313, Ural State University, Ural, 1995, English translation by Kluwer Academic Publishers.
[21] G.N. Milstein, Yu.M. Repin, M.V. Tretyakov, Mean-Square Symplectic Methods for Hamiltonian Systems with Multiplicative Noise, Preprint 670, Weierstraß-Institut für Angewandte Analysis und Stochastik, Berlin, Germany, 2001.
[22] G.N. Milstein, Yu.M. Repin, M.V. Tretyakov, Symplectic integration of Hamiltonian systems with additive noise, SIAM J. Numer. Anal. 39 (2002) 2066–2088.
[23] X. Meng, C.-W. Shu, B. Wu, Optimal error estimates for discontinuous Galerkin methods based on upwind-biased fluxes for linear hyperbolic equations, Math. Comput. 85 (2016) 1225–1261.
[24] Z. Sun, Y. Xing, On structure-preserving discontinuous Galerkin methods for Hamiltonian partial differential equations: energy conservation and multi-symplecticity, J. Comput. Phys. 419 (2020) 109662.
[25] Z. Sun, Y. Xing, Optimal error estimates of discontinuous Galerkin methods with generalized fluxes for wave equations on unstructured meshes, Math. Comput. 90 (2021) 1741–1772.
[26] G.N. Ord, A stochastic model of Maxwell's equations in 1+1 dimensions, Int. J. Theor. Phys. 35 (1996) 263–266.
[27] W.H. Reed, T. Hill, Triangular mesh methods for the neutron transport equation, Technical report, Los Alamos Scientific Lab, N. Mex. (USA), 1973.
[28] S.M. Rytov, Y.A. Kravtsov, V.I. Tatarskii, Principles of Statistical Radiophysics: Elements and Random Fields 3, Springer, Berlin, 1989.
[29] W. Tang, Y. Sun, W. Cai, Discontinuous Galerkin methods for Hamiltonian ODEs and PDEs, J. Comput. Phys. 330 (2017) 340–364.
[30] L. Zhang, C. Chen, J. Hong, L. Ji, A review on stochastic multi-symplectic methods for stochastic Maxwell equations, Commun. Appl. Math. Comput. 1 (2019) 467–501.